


Primordial helical magnetic fields from inflation?

Alireza Talebian^{⊗,*}, Amin Nassiri-Rad,[†] and Hassan Firouzjahi^{⊗‡}
*School of Astronomy, Institute for Research in Fundamental Sciences (IPM),
 P.O. Box 19395-5531, Tehran, Iran*

 (Received 8 November 2021; accepted 8 January 2022; published 26 January 2022)

We revisit the mechanism of helical magnetogenesis during inflation with a parity-violating interaction using the formalism of stochastic inflation. One of the polarizations of the gauge field undergoes tachyonic growth, leading to the generation of helical magnetic fields. We obtain the Langevin equations associated with the electromagnetic fields, which are in the form of Ornstein-Uhlenbeck stochastic differential equations. Consequently, the tachyonic growth of the helical magnetic fields is balanced by a mean-reverting process of stochastic dynamics such that the magnetic fields settle down to an equilibrium state with the amplitude smaller than what is obtained in the absence of the stochastic noises. Working in the parameter space of the model where both the backreaction and the strong coupling problems are under control, the model does not provide a large enough seed to be amplified by the galactic dynamo as the source of the magnetic fields observed on cosmological scales.

DOI: [10.1103/PhysRevD.105.023528](https://doi.org/10.1103/PhysRevD.105.023528)

I. INTRODUCTION

Magnetic fields are present throughout the observable Universe: in stars, in the interstellar medium, in galaxies, and in clusters of galaxies. However, from an astrophysical point of view, the origin of magnetic fields on large cosmological scales is still mysterious. On all scales, an initial magnetic seed with sufficient strength is needed. Seed fields may be generated with different strengths due to a variety of processes [1,2]. There has been a lot of debate about whether seed fields can be produced by battery mechanisms (charge separation processes, separation of charges, and production of currents) during galaxy and cluster formation [3,4], or whether seed fields with a primordial origin are needed. Both scenarios are currently under active consideration [5–9]. Several mechanisms have been proposed for the origin of primordial seed fields, ranging from cosmological phase transitions [10] to the inflationary production of magnetic fields [11–24]. For a review of proposed scenarios, we refer the reader to Refs. [8,25,26].

We are interested in two classes of observations at two different scales that put constraints on magnetogenesis scenarios. The first is galactic magnetic fields (GMFs) with amplitudes of the order of $\sim\mu\text{G}$, and the second is the lower bound of 10^{-16} G on intergalactic magnetic fields (IGMFs) on Mpc scales. The mechanism behind the generation of magnetic fields remains mysterious, not only on scales with

a large correlation length, $L_B \gtrsim 1$ Mpc [7,27], but also on smaller scales, $L_B \lesssim 1$ Mpc. The origin of an initial magnetic seed with sufficient strength (to be amplified by either astrophysical or primordial processes) is still unknown.

While astrophysical origins for the observed magnetic fields are not excluded, the detection of magnetic fields with a correlation length $\gtrsim 1$ Mpc in cosmic voids [28–32] has rekindled interest in the construction of inflationary mechanisms of magnetogenesis. Cosmic inflation allows us to imagine that quantum fluctuations of magnetic fields are stretched beyond the horizon, which later seeds the observed magnetic fields with a very large coherent length [23,24], an opportunity which is not available in models of the early Universe without inflation. However, the conformal invariance of Maxwell theory implies that magnetic fields cannot be generated in an expanding Universe [23,24,33]. A simple way to generate the magnetic fields during inflation is to introduce an interaction between the inflaton and the electromagnetic fields that breaks the conformal invariance. Since the violation of gauge invariance generally gives rise to ghostlike instabilities [34,35], the mechanisms that preserve gauge invariance while breaking the conformal invariance have gained most of the attention.

The best-studied model of inflationary magnetogenesis is the so-called Ratra model¹ [24,36–50], in which an interaction between the electromagnetic field and the inflaton (or a spectator) field is introduced. The action contains the nonminimal coupling $I^2(\phi)F_{\mu\nu}F^{\mu\nu}$, where ϕ is

*talebian@ipm.ir
 †amin.nassiriraad@ipm.ir
 ‡firouz@ipm.ir

¹For conciseness, we refer to this model as the “Ratra model.”

the inflaton field, $F_{\mu\nu}$ is the electromagnetic field strength, and the conformal coupling $I(\phi)$ is added to break the conformal invariance. The elementary versions of the model suffer from two main problems: the strong coupling problem, and the backreaction problem [36,38–42]. For some ranges of the parameter space, both problems are bypassed, but in those cases the generated magnetic field is not stronger than 10^{-32} G [39] at 1 Mpc today. Another well-studied mechanism is the combination of a Ratra-like coupling with an axionlike coupling—i.e., $L \supseteq I^2(\phi)(F^{\mu\nu}F_{\mu\nu} + \gamma F^{\mu\nu}\tilde{F}_{\mu\nu})$ —in which γ is a constant. This Lagrangian generates helical magnetic fields. After inflation and before recombination, as the plasma is highly turbulent with a large Reynolds number, the inverse cascade process plays a significant role in the subsequent evolution of magnetic fields and their coherence length [51]. Taking into account the constraints from non-Gaussianities [52] and induced gravitational waves [53] in this model, the scenario can satisfy the observational lower bounds on IGMFs while providing a seed for the galactic dynamo to generate GMFs. Caprini and Sorbo [53] have claimed that the model can provide a magnetic field amplitude of the order of 10^{-19} G on the Mpc scale [53]. This comes at the price of a low energy scale of inflation, ranging from 10^5 to 10^{10} GeV.

In our previous work [54], we have studied the effects of electromagnetic noises on the generation of primordial magnetic fields in the Ratra-like model using the mechanism of stochastic inflation. It was shown therein that the stochastic effects can play important roles which affect the previous estimations on the amplitude of backreactions on the inflation dynamics, yielding large enough seeds for magnetogenesis. Motivated by the nontrivial contributions of stochastic noises on the system containing gauge fields, one may expect that the stochastic effects can play important roles in axion magnetogenesis setup as well. In this paper, we revisit the axion magnetogenesis model, taking into account the stochastic noises of the electromagnetic fields. We show that the stochastic effects indeed can significantly modify the previous results for helical magnetogenesis.

The rest of the paper is organized as follows: In Sec. II, the magnetogenesis mechanism in a model of inflation with the parity-violating interaction is reviewed, and the relevant results of previous works—e.g., Refs. [52,53]—are presented. In Sec. III, we revisit the setup, taking into account stochastic noises, and we derive the Langevin equations of the electric and magnetic fields and investigate the parameters of the model. In Sec. IV, we discuss the observational constraints on the magnetic fields at the present time and search the parameter space of the model where the constraints are satisfied. Section V is devoted to the summary and conclusions, while many technicalities associated with the stochastic noises and their correlations and the cosmological evolution of the magnetic fields are relegated to the Appendixes.

II. THE MODEL

The setup is based on a hybrid of the Ratra and axion models. The electromagnetic Lagrangian density \mathcal{L}_{EM} consists of a $U(1)$ gauge field A_μ coupled to an axionic inflaton field ϕ via

$$\mathcal{L}_{\text{EM}} = -\frac{1}{4}I^2(\phi)\left(F_{\mu\nu}F^{\mu\nu} + \frac{\gamma}{2}F_{\mu\nu}\tilde{F}^{\mu\nu}\right), \quad (2.1)$$

where $F_{\mu\nu} = \partial_\mu A_\nu - \partial_\nu A_\mu$ is the field strength and $\tilde{F}^{\mu\nu} \equiv \frac{\epsilon^{\mu\nu\alpha\beta}}{2\sqrt{-g}}F_{\alpha\beta}$ is its dual, with $\epsilon^{0123} = 1$. Here, we choose the constant parameter $\gamma < 0$ without loss of generality. Since the energy density of the electromagnetic field is exponentially diluted during the quasi-de Sitter inflationary expansion, the conformal coupling $I(\phi)$ is added to break the conformal invariance. With this conformal coupling, the energy is continuously pumped from the inflaton sector to the gauge field sector, so the electromagnetic energy density survives the exponential dilution. Although the conformal coupling is a function of ϕ , the latter itself is a function of time, so we consider the following phenomenological ansatz for the conformal coupling:

$$I(\tau) = I_e \left(\frac{\tau}{\tau_e}\right)^n, \quad (2.2)$$

where the conformal time τ is related to the cosmic time t via the scale factor a as in $dt = a d\tau$, τ_e and I_e are the corresponding terminal values at the end of inflation. This coupling was employed extensively in the context of anisotropic inflation [55–62] and the generation of primordial magnetic fields during inflation [24,36–50]. The spectral index of the magnetic field is controlled by the parameter n , so a scale-invariant magnetic field can be obtained for the cases $n = 3$ or $n = -2$.

To study magnetogenesis in the presence of the Lagrangian \mathcal{L}_{EM} [Eq. (2.1)], we start with the following action:

$$S = \int d^4x \sqrt{-g} \left[\frac{M_{\text{Pl}}^2}{2} R - \frac{1}{2} g^{\mu\nu} \partial_\mu \phi \partial_\nu \phi - V(\phi) + \mathcal{L}_{\text{EM}} \right], \quad (2.3)$$

in which R is the Ricci scalar and $M_{\text{Pl}} \equiv (8\pi G)^{-\frac{1}{2}}$ is the reduced Planck mass with G being the Newton constant.

We assume that the electromagnetic fields are purely excited quantum mechanically. This means that the electromagnetic fields have no background components so they do not contribute to the background energy density. The background is given by a spatially flat, Friedmann-Lemaître-Robertson-Walker (FLRW) universe, described by the line element

$$ds^2 = a^2(\tau)(-d\tau^2 + d\mathbf{x} \cdot d\mathbf{x}), \quad (2.4)$$

in which the relation $a \simeq -(H\tau)^{-1}$ can be used with good accuracy, where H is the Hubble expansion rate during inflation.

It is more convenient to work in the temporal Coulomb gauge $A_0 = \partial_i A_i = 0$ and define the electric and magnetic fields as

$$E_i \equiv -I \frac{\partial_\tau A_i}{a^2}, \quad B_i \equiv I \frac{\epsilon_{ijk} \partial_j A_k}{a^2}. \quad (2.5)$$

With the above definitions, the Friedmann and Klein-Gordon (KG) equations take the following form:

$$3M_{\text{Pl}}^2 H^2 = \frac{1}{2} \dot{\phi}^2 + V + \rho_{\text{EM}},$$

$$\rho_{\text{EM}} \equiv \frac{1}{2} (E^2 + B^2), \quad (2.6)$$

$$\ddot{\phi} + 3H\dot{\phi} - \frac{\nabla^2}{a^2} \phi + V_{,\phi} = S_{\text{EM}},$$

$$S_{\text{EM}} \equiv \frac{1}{\phi a} \frac{I'}{I} (E^2 - B^2 - 2\gamma \mathbf{E} \cdot \mathbf{B}), \quad (2.7)$$

where a dot (prime) denotes the derivative with respect to the cosmic time t (conformal time τ). Note that ρ_{EM} represents the electromagnetic field energy density, while S_{EM} is the backreaction source of the electromagnetic fields on the KG field equation.

Finally, the Maxwell equations with the Bianchi identities read as

$$\dot{\mathbf{B}} + H(2+n)\mathbf{B} = -\frac{\mathbf{V} \times \mathbf{E}}{a}, \quad (2.8)$$

$$\dot{\mathbf{E}} + \gamma \dot{\mathbf{B}} + H(2-n)(\mathbf{E} + \gamma \mathbf{B}) = -\frac{\mathbf{V} \times (\mathbf{B} + \gamma \mathbf{E})}{a}. \quad (2.9)$$

There are two important issues which should be taken into account when constructing a scenario of magnetogenesis during inflation: the strong coupling problem and the electric field backreaction problem. Looking at the electromagnetic action, we realize that the gauge coupling is $I(\phi)^{-1}$, so in order for the perturbative field theory to be trusted, we require that $I(\phi) \geq 1$ for all time during inflation. With the phenomenological ansatz given in Eq. (2.2), we need $n > 0$ in order to avoid the strong coupling problem. Furthermore, we set $I_e = 1$ in Eq. (2.2) such that we recover the standard Maxwell theory at the end of inflation when the inflaton decays through the (p) reheating process. The backreaction problem, on the other hand, is associated with the fact that for some regions of parameter space, the electric field is enhanced so efficiently that its energy density can dominate over the inflaton

potential, terminating inflation prematurely [39]. As studied in Ref. [54], to avoid the backreaction and the strong coupling problems, we require $\frac{1}{2} < n < 2$, which will be considered in this work as well. As studied in Ref. [54] (see also Refs. [63,64]), stochastic effects have important implications for these two problems. The stochastic noises cause the solutions of electromagnetic fields to settle down to an equilibrium state in such a way that (for an acceptable range of parameter space) not only are the backreaction effects under control, but also an acceptable amount of magnetic field is generated.

To have the backreaction effects under control, we assume that the gauge field contributions do not destroy the dynamics of the inflaton field or the background geometry given in Eqs. (2.6) and (2.7), respectively. This means that

$$\Omega_{\text{EM}} \equiv \frac{\rho_{\text{EM}}}{3M_{\text{Pl}}^2 H^2} \ll 1, \quad (2.10)$$

$$R_S \equiv \left| \frac{S_{\text{EM}}}{3H\dot{\phi}} \right| \ll 1. \quad (2.11)$$

Both of the above conditions must be satisfied during inflation. We check these conditions in the context of stochastic formalism and specify the allowed regions of the parameter space.

To study the behavior of electromagnetic fields in this model, we look at the quantum fluctuations of the gauge field during inflation. Defining the canonical field as $\tilde{A}_i \equiv I A_i$ and going to the Fourier space, we expand \tilde{A}_i in terms of the creation and annihilation operators $a_{\mathbf{k}}$ and $a_{\mathbf{k}}^\dagger$ as follows:

$$\tilde{A}_i = \sum_{\lambda=\pm} \int \frac{d^3 k}{(2\pi)^3} e_i^\lambda(\mathbf{k}) (v_{k,\lambda}(\tau) a_{\mathbf{k},\lambda} + v_{k,\lambda}^*(\tau) a_{-\mathbf{k},\lambda}^\dagger) e^{i\mathbf{k} \cdot \mathbf{x}}, \quad (2.12)$$

in which $v_{k,\lambda}$ is the mode function and e^λ are the circular polarization vectors satisfying the relations

$$\begin{aligned} \mathbf{e}_\lambda(\hat{\mathbf{k}}) \cdot \mathbf{e}_{\lambda'}^*(\hat{\mathbf{k}}) &= \delta_{\lambda\lambda'}, \\ \hat{\mathbf{k}} \cdot \mathbf{e}^\lambda(\hat{\mathbf{k}}) &= 0, \\ i\hat{\mathbf{k}} \times \mathbf{e}^\lambda &= \lambda \mathbf{e}^\lambda, \\ \mathbf{e}_\lambda(\hat{\mathbf{k}}) &= \mathbf{e}_\lambda^*(-\hat{\mathbf{k}}), \\ \sum_{\lambda=\pm} \mathbf{e}_i^\lambda(\hat{\mathbf{k}}) \mathbf{e}_j^{\lambda*}(\hat{\mathbf{k}}) &= \delta_{ij} - \hat{k}_i \hat{k}_j. \end{aligned} \quad (2.13)$$

Substituting Eq. (2.12) into the action and using ansatz (2.2), the equation for the mode function is given by

$$v''_{k,\lambda} + \left(k^2 + 2\lambda\xi \frac{k}{\tau} - \frac{n(n-1)}{\tau^2} \right) v_{k,\lambda} = 0, \quad \xi \equiv -n\gamma. \quad (2.14)$$

Here we have defined the instability parameter $\xi > 0$ [remember that we have chosen $\gamma < 0$ in the Lagrangian of Eq. (2.1)]. As we shall see, ξ is one key parameter of the model which controls the strength of tachyonic instability for the gauge field perturbations. In the previous works of magnetogenesis based on the setup of Eq. (2.1) [53,65], ξ has been taken to be in the range $\xi \sim \mathcal{O}(10)$.

The mode function $v_{k,\lambda}$ satisfying Eq. (2.14) evolves in three stages as follows: During early times, $\tau \rightarrow -\infty$, the ultraviolet term k^2 dominates, and the gauge quanta are in their Bunch-Davies vacuum. Later on, before horizon crossing, the term proportional to ξ becomes important for the subhorizon modes with $|k\tau| \lesssim \xi$. Since $\tau < 0$ during inflation, the mode function with positive helicity is exponentially amplified, whereas the mode of opposite helicity does not experience such an amplification. In order for an efficient enhancement to take place, one requires $\xi \gg 1$, in which a net chirality in the gauge field perturbations is generated. Finally, as $\tau \rightarrow 0$, the last term in the parenthesis takes over, as in conventional models of inflation based on scalar field dynamics.

The above three-stage processes can be addressed by a function with three arguments such as the Whittaker functions. Actually, the solutions to this equation are given by a linear combination of Whittaker functions $W_{\mu,\nu}(z)$ and $M_{\mu,\nu}(z)$ with the coefficients determined by the initial conditions. Imposing the standard Bunch-Davies solutions at early times² $-k\tau \rightarrow \infty$, the solution of Eq. (2.14) is given by

$$v_{k,\lambda}(\tau) = \frac{e^{\frac{\lambda\pi\xi}{2}}}{\sqrt{2k}} W_{\mu,\nu}(2ik\tau), \quad \mu \equiv -i\lambda\xi, \quad \nu \equiv n - 1/2. \quad (2.15)$$

For $\gamma = 0$, it is easy to check that the above mode function coincides with the well-known mode function in terms of the Hankel functions³ used in earlier studies, such as in Ref. [54].

During the second stage, in which the second term in the parenthesis in Eq. (2.14) dominates, the subhorizon modes with $\lambda = +$ are amplified. In the regime $|k\tau| \ll \xi$, the solution (2.15) is approximated to [53,66]

$$v_k^+(\tau) \simeq \sqrt{-\frac{2\tau}{\pi}} e^{\pi\xi} K_{2\nu}(\sqrt{8\xi|k\tau|}), \quad |k\tau| \ll \xi, \xi \gg 1, \quad (2.16)$$

² $W_{\mu,\nu}(z) \rightarrow z^\mu e^{-z/2}$ for $z \rightarrow \infty$.

³ $W_{0,\nu}(z) = \frac{\sqrt{\pi z}}{2} i^{\nu+1} H_\nu^{(1)}\left(\frac{iz}{2}\right)$, in which $H^{(1)}(x)$ is the Hankel function of the first kind.

where K_ν is the modified Bessel function of the second kind. Subsequently, for $|k\tau| \ll 1/\xi$, we obtain

$$v_k^+(k, \tau) \simeq \sqrt{-\frac{\tau}{2\pi}} e^{\pi\xi} \Gamma(2n-1) |2\xi k\tau|^{-(n-1/2)}, \quad |k\tau| \ll 1/\xi \ll 1. \quad (2.17)$$

As seen, the amplitude of the gauge field is exponentially enhanced via the instability parameter ξ .

Our first task is to calculate the amplitude of the generated magnetic field, its correlation length, and the spectral index at the time of the end of inflation $\tau = \tau_e$. In Appendix A, we have defined these quantities in Eqs. (A12), (A11), and (A14), denoted by $B(\tau_e)$, $L(\tau_e)$, and n_B , respectively. Assuming an instantaneous reheating scenario after inflation and denoting the values of $B(\tau_e)$ and $L(\tau_e)$ in the absence of stochastic effects by \bar{B}_{rh} and \bar{L}_{rh} , the intensity of the magnetic field is found to be⁴ [53]

$$\bar{B}_{\text{rh}} \simeq 1.9 \times 10^{53} \text{ G} \left(\frac{H}{M_{\text{Pl}}} \right)^2 e^{\pi\xi} \xi^{-5/2} \sqrt{\Gamma(4+2n)\Gamma(6-2n)}, \quad (2.18)$$

while the correlation scale is given by [53]

$$\bar{L}_{\text{rh}} \simeq \frac{18\pi}{(3+2n)(5-2n)} \frac{\xi}{H}, \quad (2.19)$$

and the magnetic spectral index on large scales reads as

$$n_B = \frac{5}{2} - \left| n - \frac{1}{2} \right|. \quad (2.20)$$

Therefore, the cases $n = 3$ and $n = -2$ lead to magnetic fields with scale-invariant spectra. As mentioned before, to keep the backreaction and the strong coupling problems under control, we require $\frac{1}{2} < n < 2$, so Eq. (2.20) simplifies to

$$n_B = 3 - n. \quad (2.21)$$

For large enough values of ξ , the gauge field perturbations can induce sizeable gravitational waves [53] and non-Gaussianities [52] which are under observational constraints on CMB scales [67]. Therefore, the tensor-to-scalar ratio r_t and the equilateral configuration non-Gaussianity $f_{\text{NL}}^{\text{equil}}$ can be used to express the Hubble parameter H in terms of the model parameters n and ξ . According to Refs. [52,53], we have

⁴We estimate the reduced Planck mass in units of gauss as $M_{\text{Pl}}^2 \simeq 3 \times 10^{56} \text{ G}$.

$$\frac{H}{M_{\text{Pl}}} \simeq e^{-\pi\xi} \left(\frac{r_t \mathcal{P}_\zeta}{p^t(n)} \right)^{1/4} \xi^{3/2}, \quad (2.22)$$

$$\frac{H}{M_{\text{Pl}}} \simeq e^{-\pi\xi} \left(\frac{f_{\text{NL}}^{\text{equil}} \mathcal{P}_\zeta^2}{p^f(n)} \right)^{1/6} \xi^{3/2}, \quad (2.23)$$

where $\mathcal{P}_\zeta \simeq 2.1 \times 10^{-9}$ is the amplitude of the scalar perturbations, and the functions $p^t(n)$ and $p^f(n)$ are defined in Refs. [52,53], respectively. The above relations are obtained for $\xi \sim \mathcal{O}(10)$, which leads to a very small energy scale of inflation. However, in the following analysis and in the presence of stochastic noises, we show that for $\xi \sim \mathcal{O}(10)$ there are significant backreactions on the Klein-Gordon equation which spoil the inflationary dynamics. To bypass this issue, the upper bound $\xi \lesssim 3$ must be considered, which is consistent with the findings of Refs. [66,68]. We confirm that for $\xi \lesssim 3$, the usual vacuum tensor perturbations have the dominant contribution in r_t , so that the energy scale of inflation can take higher values, in contrast to the conclusion of Ref. [52].

The above was a brief review of inflationary magnetogenesis in the setup with the action of Eq. (2.3) in the conventional approach and in the absence of stochastic effects. In the next section, we revisit these conclusions in the context of stochastic inflation.

III. STOCHASTIC ANALYSIS

In this section, we study the magnetogenesis mechanism, taking into account the effects of stochastic noises. We employ the formalism of stochastic inflation, which is an effective theory for the long-wavelength modes [69–71]. In this formalism, the quantum fields are decomposed into long- and short-wavelength modes. The long modes are the coarse-grained perturbations on super-Hubble scales, while the short modes act as the stochastic forces for the evolution of the long modes at the time when they leave the Hubble horizon. For light scalar perturbations, the amplitude of these stochastic noises is $H/2\pi$, while for the electromagnetic perturbations they show more nontrivial properties [54,64].

To perform stochastic analysis, we decompose the electric and magnetic fields into long and short modes [72–74]. Denoting these fields collectively as $X = E_i, B_i$, we write

$$X = X_1 + \sqrt{\hbar} X_s, \quad (3.1)$$

where the IR (X_1) and UV (X_s) parts are decomposed via the step function Θ as

$$X_{s,i}(\mathbf{x}, t) = \int \frac{d^3k}{(2\pi)^3} \Theta(\pm k \mp k_c) e^{i\mathbf{k}\cdot\mathbf{x}} \hat{X}_k(t), \quad (3.2)$$

where the upper (lower) sign in Eq. (3.2) corresponds to the short (long) modes and $k_c \equiv \varepsilon a(t)H$, with $\varepsilon \ll 1$ being a

small cutoff parameter. In addition, $\hat{X}_\mathbf{k}$ is the quantum operator expanded as

$$\begin{aligned} \hat{X}_\mathbf{k} &= a_\mathbf{k} X_k + a_{-\mathbf{k}}^\dagger X_{-k}, \\ [a_{\mathbf{k}'\lambda'}, a_{\mathbf{k}\lambda}^\dagger] &= (2\pi)^3 \delta_{\lambda\lambda'} \delta^3(\mathbf{k} - \mathbf{k}'), \end{aligned} \quad (3.3)$$

where $a_\mathbf{k}$ and $a_\mathbf{k}^\dagger$ are the usual ladder operators and X_k is the Fourier component of the fields. Note that these ladder operators are the same for the electric, magnetic, and gauge fields.

To perform stochastic calculus, it is more convenient to use the dimensionless variables $\mathcal{X} = \mathcal{B}, \mathcal{E}$ associated with the long-mode perturbations of the electric and magnetic fields defined via

$$\mathcal{X} \equiv \frac{X_1}{HM_{\text{Pl}}}. \quad (3.4)$$

Substituting Eq. (3.1) into Eqs. (2.8) and (2.9) and expanding for the long modes—i.e., $k < k_c$ —we find the Langevin equations for the electric and magnetic fields. More specifically, neglecting the terms proportional to the gradients of the fields or the slow-roll parameters, we obtain

$$\mathcal{B}'_i = -(2+n)\mathcal{B}_i + \hat{\sigma}_i^{\mathcal{B}}(N), \quad (3.5)$$

$$\mathcal{E}'_i = -(2-n)\mathcal{E}_i + 2n\gamma\mathcal{B}_i + \hat{\sigma}_i^{\mathcal{E}}(N), \quad i = 1, 2, 3, \quad (3.6)$$

where the index i represents the spatial components of the fields, and the prime here and below denotes the derivative with respect to the e -folding number, $dN = Hdt$. The quantum noises $\hat{\sigma}^X(N)$, emerging from the UV modes, are defined as

$$\hat{\sigma}^X(\mathbf{x}, t) = -\frac{dk_c}{dt} \int \frac{d^3k}{(2\pi)^3} \delta(k - k_c) e^{i\mathbf{k}\cdot\mathbf{x}} \hat{\mathcal{X}}_k(t). \quad (3.7)$$

Both the electric and magnetic noises are determined via the mode function of the gauge field [Eq. (2.15)]. We are ultimately interested in the superhorizon behavior of the above mode function, which controls the behavior of quantum noises $\hat{\sigma}^X$. The properties of the electromagnetic noises and their correlations are studied in Appendix B. Here, we rewrite Eq. (B9) in terms of the number of e -folds as

$$\langle \hat{\sigma}_i^X(N_1) \hat{\sigma}_j^X(N_2) \rangle = D_X^2 \delta_{ij} \delta(N_1 - N_2), \quad (3.8)$$

where D_X is the diffusion coefficient defined by

$$D_X^2 \equiv \frac{1}{18\pi^2} \frac{dk_c^3}{dN} \sum_\lambda |X_\lambda(N, k_c)|^2. \quad (3.9)$$

Using the small argument behavior of the mode function [Eq. (2.15)],⁵ the diffusion coefficients have been calculated in Eq. (B19), which for $\xi \gg 1$ yields⁶

$$D_B \simeq \frac{e^{\pi\xi} \sqrt{\xi} \Gamma(2n-1)}{\pi\sqrt{3\pi}} \frac{H}{2^n M_{\text{Pl}}} \varepsilon^{n_B}, \quad (3.10)$$

$$D_E = D_B \frac{(2n-1)}{\varepsilon}, \quad (3.11)$$

where the magnetic field spectral index is defined in Eq. (2.21): $n_B = 3 - n$.

There are some important comments to discuss here. First, the amplitude of the diffusion coefficient of the electric field is stronger than that of the magnetic field by a factor ε^{-1} . This is the reason why it is always the backreaction from the electric field that spoils the slow-roll inflation. Second, while the parameter ε is employed in our analysis as a bookkeeping parameter to separate the long and short modes, it appears on the diffusion coefficients as well. Curiously, the dependences on ε for both diffusion coefficients are exactly determined by the scale dependency of each perturbations—i.e., D_B (D_E) is independent of ε when $n = 3$ ($n = 2$). As we mentioned in the previous section, it is a well-known result that the magnetic (electric) fields are scale invariant for $n = 3$ ($n = 2$).

Since the quantum nature of these noises disappears for $\varepsilon \ll 1$ (see Appendix A for more details), one can express the quantum noises $\hat{\sigma}^X(N)$ in terms of the classical normalized white noise $\sigma(N)$ as

$$\hat{\sigma}_i^X(N) \equiv D_X \sigma_i(N), \quad (3.12)$$

where

$$\begin{aligned} \langle \sigma_i(N) \rangle &= 0, \\ \langle \sigma_i(N_1) \sigma_j(N_2) \rangle &= \delta_{ij} \delta(N_1 - N_2). \end{aligned} \quad (3.13)$$

Now, we define a three-dimensional (3D) Wiener (or Brownian) process with the components W_i associated with the noise σ_i via

$$dW_i(N) \equiv \sigma_i(N) dN, \quad (3.14)$$

and we rewrite the stochastic differential equations (3.5) and (3.6) in the following form:

$$d\mathcal{B}_i = -(2+n)\mathcal{B}_i dN + D_B dW_i(N), \quad (3.15)$$

$$d\mathcal{E}_i = -(2-n)\mathcal{E}_i + 2n\gamma\mathcal{B}_i dN + D_E dW_i(N). \quad (3.16)$$

The second terms in each of the above equations represent the effect of the random noises, while the first terms, proportional to dN , represent the classical drift term. For $1/2 < n < 2$, both of the above classical drift terms are negative, and the system is in the form of Ornstein-Uhlenbeck (OU) stochastic differential equations. The main feature of the OU process is that the frictional drift force can be balanced by the random force, so the stochastic fields \mathcal{B} and \mathcal{E} admit equilibrium states with long-term means and bounded variances (a mean-reverting process). To be more precise, an OU process is a stationary Gauss-Markov process in which there is the tendency for the system to drift toward the mean value, with a greater attraction when the process is further away from the mean. For this process, the explicit dependence of the mean on the initial conditions is washed out over time, and the system can be fully described by the drift and the diffusion coefficients.

To solve the coupled Langevin equations (3.15) and (3.16), we go to a basis in which the equations are decoupled (see Appendix C for more details). We have assumed that the electromagnetic fields are purely excited quantum mechanically. This means that the electromagnetic fields have no background components, so we set the initial conditions for the electromagnetic fields to zero in Eqs. (C11) and (C12), obtaining

$$\mathcal{B}_i(N) = D_B \int_0^N e^{(n+2)(N'-N)} \sigma_i(N') dN', \quad (3.17)$$

$$\mathcal{E}_i(N) = -\gamma\mathcal{B}_i(N) + (D_E + \gamma D_B) \int_0^N e^{-(n-2)(N'-N)} \sigma_i(N') dN'. \quad (3.18)$$

Our main goal is to calculate various cases of the electric and magnetic correlation function (stochastic averages). Using the following properties of the stochastic integrals [75],

$$\begin{aligned} \left\langle \int_0^{N'} G(N) dW(N) \int_0^{N'} F(N) dW(N') \right\rangle \\ = \int_0^{N'} G(N) F(N) dN, \end{aligned} \quad (3.19)$$

$$\left\langle \int_0^{N'} G(N) dW(N) \right\rangle = 0, \quad (3.20)$$

we can calculate the mean and the variance associated with $\mathcal{B}_i(N)$ and $\mathcal{E}_i(N)$. More specifically,

$$\langle \mathcal{B}_i \rangle = \langle \mathcal{E}_i \rangle = 0, \quad (3.21)$$

$$\langle \mathcal{B}_i^2(N) \rangle = \frac{D_B^2}{2(n+2)} (1 - e^{-2(n+2)N}), \quad (3.22)$$

⁵ $W_{\mu,\nu}(z) \rightarrow z^{1/2-\nu} \Gamma(2\nu) / \Gamma(\nu - \mu + 1/2)$ for $z \rightarrow 0$.

⁶We have used the approximation $|\Gamma(x + iy)|^2 \simeq \pi / (y \sinh(\pi y))$ for $y \gg x$.

$$\begin{aligned} \langle \mathcal{E}_i^2(N) \rangle &= \gamma^2 \langle \mathcal{B}_i^2(N) \rangle - \frac{\gamma}{2} D_B (D_E + \gamma D_B) (1 - e^{-4N}) \\ &+ (D_E + \gamma D_B)^2 \times \begin{cases} \frac{1 - e^{-2(2-n)N}}{2(2-n)}, & n \neq 2 \\ N, & n = 2 \end{cases}. \end{aligned} \quad (3.23)$$

A. Backreaction condition

Having calculated $\langle \mathcal{B}_i^2(N) \rangle$, we can go ahead to look for the predictions of the model for the primordial magnetogenesis. However, before that, we should check the backreaction conditions induced on the background dynamics, parametrized by Eqs. (2.10) and (2.11). For the case $\xi < 1$, there is no tachyonic instability from the parity-violating term and, as shown in Ref. [54], the system is under control for the range $\frac{1}{2} < n \leq 2$. However, in the current setup with $\xi > 1$, new backreactions from the tachyonic enhancement of the + mode of the gauge field can be induced. As we demonstrate below, for keeping the backreactions under control, one actually requires $\xi \lesssim 3$.

Using the definitions of \mathcal{E} and \mathcal{B} in Eq. (3.4), the backreaction constraints [Eqs. (2.10) and (2.11)] are given by

$$\Omega_{\text{EM}} = \frac{1}{6} (\mathcal{E}^2 + \mathcal{B}^2) \ll 1, \quad (3.24)$$

$$R_S = \frac{n}{6\epsilon_\phi} (\mathcal{E}^2 - \mathcal{B}^2 - 2\gamma\mathcal{E} \cdot \mathcal{B}) \ll 1, \quad (3.25)$$

where the magnitudes of the fields are given by $\mathcal{X} \equiv (\sum_{i=1}^3 \mathcal{X}_i^2)^{1/2}$ for $\mathcal{X} = \mathcal{B}, \mathcal{E}$, and the inflaton slow-roll parameter ϵ_ϕ is defined as

$$\epsilon_\phi \equiv \frac{\dot{\phi}^2}{2M_{\text{Pl}}^2 H^2}. \quad (3.26)$$

Note that in general, ϵ_ϕ differs from the Hubble slow-roll parameter $\epsilon_H \equiv -\dot{H}/H^2$. Combining Eqs. (2.6) and (2.7), we find that

$$\epsilon_H = \epsilon_\phi + 2\Omega_{\text{EM}} - \frac{2n\gamma}{3} \mathcal{E} \cdot \mathcal{B}. \quad (3.27)$$

As seen, these two slow-roll parameters do not coincide in general, especially when the backreaction effects are significant.

Now, in order to estimate the backreaction effects, we note that the constraint of Eq. (3.25) is stronger than Eq. (3.24) by a slow-roll factor $\Omega_{\text{EM}} \simeq \epsilon_\phi R_S$. This means that the backreactions from the electromagnetic field affect the dynamics of the inflaton field sooner than the background expansion rate. Therefore, the fractional energy density of the electromagnetic fields is subdominant, and the constraint $R_S \ll 1$ must be checked first. For a fixed cutoff parameter ϵ , this constraint leads to a limited

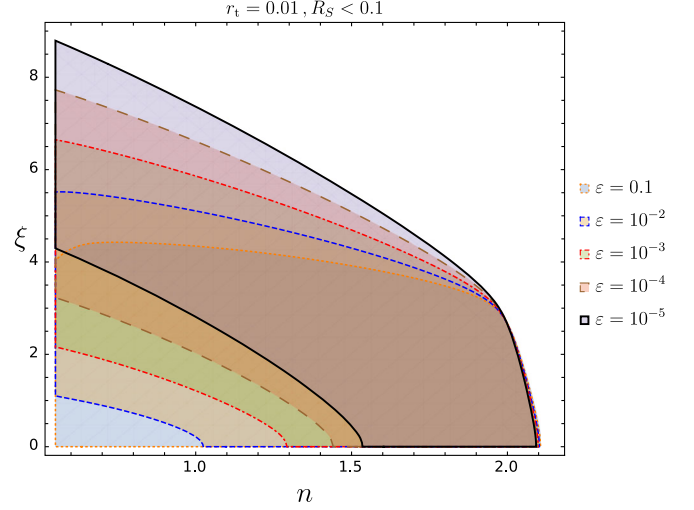


FIG. 1. The allowed parameter space of $\xi - n$ where the backreaction effects are not significant—i.e., $R_S < 0.1$. To be conservative, for all values of ϵ , the backreactions can be neglected in the interval $\frac{1}{2} < n < 2$ when $\xi \lesssim 3$.

parameter space for n and ξ . In Fig. 1, we have plotted the allowed regions where the condition $R_S \ll 1$ is satisfied in the parameter space $\xi - n$. It is found that for the entire range $1/2 < n < 2$, we require $\xi \lesssim 3$ in order for the backreaction $R_S \ll 1$ to be satisfied. Note that the constraint $\xi \lesssim 3$ is obtained in Refs. [66,68] as well. In this range of parameter space, we can safely consider $\epsilon_H \simeq \epsilon_\phi$ to a very good accuracy.

Now, let us consider a slightly different setup, as studied in Ref. [52], in which a spectator field σ other than the inflaton field is coupled to the $F\tilde{F}$ term and $I = I(\sigma)$. Then, one can parametrize the backreaction of the gauge field on the KG equation of the test field as

$$R_S^\sigma \equiv \frac{n}{6\epsilon_\sigma} (\mathcal{E}^2 - \mathcal{B}^2 - 2\gamma\mathcal{E} \cdot \mathcal{B}), \quad (3.28)$$

where the test field slow-roll parameter is defined as

$$\epsilon_\sigma \equiv \frac{\dot{\sigma}^2}{2M_{\text{Pl}}^2 H^2}. \quad (3.29)$$

Demanding that the test field remain subdominant with respect to the inflaton field, we require $\epsilon_\sigma < \epsilon_\phi$. Therefore, we find that $R_S^\sigma > R_S$, so that the maximum value of ξ allowed is even less than in the case when the running field is the inflaton field itself. In other words, the backreaction is stronger for the test field σ coupled to the gauge field.

In summary, we need $\xi \lesssim 3$ to meet the backreaction condition. This is in contrast with the conclusion of Refs. [52,53], in which ξ can take values in the range $\xi \sim 10-20$ by fine-tuning the value of H/M_{Pl} to a very small value, say $H/M_{\text{Pl}} \sim 10^{-20}$, to get the desired value of

the observed magnetic fields. This value for the Hubble parameter during inflation leads to $\epsilon_\phi \sim 10^{-32}$, which violates the backreaction constraint Eq. (95) of Ref. [52] even for an inflaton field.

B. Equilibrium state

We see from Eq. (3.22) that the magnetic field experiences an equilibrium state in which the second term in the bracket falls off exponentially [54]. Note that this is because the magnetic field equation [Eq. (3.15)] is in the form of an OU stochastic differential equation where the classical drift term with a negative coefficient is balanced by the diffusion coefficient term.

The time when the magnetic field reaches its equilibrium is estimated as [54]

$$N_{\text{eq}}^B \approx \frac{\ln 10}{n+2}, \quad (3.30)$$

when the exponential term in Eq. (3.22) falls to less than 10^{-2} . The amplitude of each component of the dimensionless magnetic fields in the stationary state is given by

$$\langle \mathcal{B}_i^2 \rangle_{\text{eq}} = \frac{D_B^2}{2(n+2)}. \quad (3.31)$$

On the other hand, the situation for the electric field is very different, as can be seen from Eq. (3.23). In the following, we study the evolution of the electric field in three different regimes: $\frac{1}{2} < n < 2$, $n = 2$, and $n > 2$.

(1) $\frac{1}{2} < n < 2$

In this regime, the electric field does not grow with time and admits an equilibrium state. The timescale when the components of the electric field reach the equilibrium state is estimated as

$$N_{\text{eq}}^E \approx \frac{2 \ln 10}{2-n}, \quad (3.32)$$

with the equilibrium magnitude

$$\begin{aligned} \langle \mathcal{E}_i^2 \rangle_{\text{eq}} &= \gamma^2 \langle \mathcal{B}_i^2 \rangle_{\text{eq}} + \frac{(D_E + \gamma D_B)^2}{2(2-n)} - \frac{\gamma D_B (D_E + \gamma D_B)}{2} \\ &\simeq \frac{D_E^2}{2(2-n)}. \end{aligned} \quad (3.33)$$

Here, we have neglected terms related to D_B in favor of D_E because D_B is smaller than D_E by a factor of ϵ , as seen from Eq. (B19).

Since the electromagnetic field falls into the stationary state for the parameter space $1/2 < n < 2$, one can use the alternative approach of a probability distribution function to study the system. This independent approach is studied in Appendix D.

(2) $n = 2$

In this special case, the electric field becomes scale invariant—i.e., D_E does not depend on ϵ —and the evolution of the components of the electric field is given by

$$d\mathcal{E}_i = -\frac{\xi D_B}{\sqrt{2}} dN + D_E dW_i(N). \quad (3.34)$$

At the end of inflation, $N \simeq 60$, the condition (3.25) is violated for $\xi \gtrsim 3$. This is the hallmark of backreaction problems induced by electric fields, as studied in previous literature using different approaches.

(3) $n > 2$

In this case, the electric field grows exponentially in time:

$$\begin{aligned} \langle \mathcal{E}_i^2(N) \rangle &\simeq \frac{(D_E + \gamma D_B)^2}{2(n-2)} e^{2(n-2)N} \\ &\simeq \frac{H^2 \xi \sinh(2\pi\xi)}{6\pi^3 M_{\text{Pl}}^2 (n-2)} \left| \frac{\Gamma(2n)}{2^n} \right|^2 \left(\frac{e^N}{\epsilon} \right)^{2(n-2)}. \end{aligned} \quad (3.35)$$

Since $\epsilon \ll 1$, $\xi \gtrsim 1$, there may be a very narrow band of the parameter space in which the backreaction conditions (3.24) and (3.25) are satisfied initially. But then the condition (3.25) is violated, and inflation is spoiled quickly. This again indicates the difficulties with the backreaction problem in this setup induced by the electric field.

Hereafter, we only consider the range $\frac{1}{2} < n < 2$ where both the magnetic and electric fields experience equilibrium states with the amplitudes in Eqs. (3.31) and (3.33), respectively. Also, as mentioned before, the amplitude of the magnetic field scales with ϵ like ϵ^{n_B} , while that of the electric field is stronger, scaling like ϵ^{n_E-1} .

Now, let us have a closer look at the parameter ϵ . As we discussed in our previous analysis [54], a lower bound on ϵ can be found in the coarse-graining process by considering the longest wavelength observable on the CMB scale, $k_{\text{CMB}} \simeq 10^{-4} \text{ Mpc}^{-1}$. On the other hand, for the magnetogenesis mechanism, we are interested in the mode k_{Mpc} associated with the physical length scale $\sim \text{Mpc}$ today. Then, the smallest value for ϵ is given by

$$\epsilon_{\text{Mpc}} \simeq \frac{k_{\text{CMB}}}{k_{\text{Mpc}}} = 10^{-5}. \quad (3.36)$$

However, a larger value for ϵ can be obtained by replacing k_{CMB} with the Planck observation's pivot scale $k_* = 0.05 \text{ Mpc}^{-1}$, which results in $\epsilon_{\text{Mpc}} \simeq 10^{-2}$. Therefore, we consider ϵ_{Mpc} in the range $10^{-2} - 10^{-5}$ in the rest of the

paper, which is also small enough to meet the criteria of the long and short decomposition of stochastic analysis.

C. Magnetic field at the end of inflation

The stationary value of the dimensionless magnetic field \mathcal{B} is given in Eq. (3.31), which will be used to calculate the amplitude of the magnetic fields at the end of inflation. For simplicity, we assume an instantaneous reheating, so we use the subscript “rh” to indicate the corresponding value at the end of inflation. To proceed further, the characteristic properties of the primordial magnetic field must be translated into the stochastic language. By “characteristic properties,” we mean the correlation scale L_{rh} , the magnetic strength B_{rh} , and the spectral index n_B , which, in the context of the conventional approach, are defined in Eqs. (A11), (A12), and (A14), respectively. The dictionary we use is as follows:

- (1) In the stochastic approach, we deal with the coarse-grained magnetic field instead of the Fourier components. Therefore, the magnetic strength [Eq. (A12)] at the end of inflation is translated to

$$B_{\text{rh}} \equiv \sqrt{\langle B_1^2 \rangle}, \quad (3.37)$$

in which $B_1 \equiv HM_{\text{Pl}}\mathcal{B}_{\text{rh}}$ is IR—the part (long mode) of the magnetic field which is defined via the relation (3.2). Since for the parameter space $1/2 < n < 2$ the magnetic field components fall into the equilibrium state [Eq. (3.31)], the coarse-grained magnetic field at the end of inflation is given by

$$\begin{aligned} B_{\text{rh}} &= HM_{\text{Pl}} \left(\sum_{i=1}^3 \langle \mathcal{B}_i^2 \rangle_{\text{eq}} \right)^{1/2} \\ &\simeq \frac{\sqrt{3}}{\sqrt{2n+4}} HM_{\text{Pl}} D_B, \end{aligned} \quad (3.38)$$

in which the relation (3.31) has been used for the component of the magnetic field in the equilibrium state. Now, using the value of D_B given in Eq. (3.10), we obtain $B_{\text{rh}} \propto H^2 e^{\pi\xi} e^{n_B}$.

- (2) The correlation scale [Eq. (A11)] can be used in the stochastic approach as well. Therefore, integrating over the modes $|k\tau| \lesssim \xi$, we obtain

$$L_{\text{rh}} \simeq \frac{18\pi}{(3+2n)(5-2n)} \frac{\xi}{H}. \quad (3.39)$$

This scale is roughly given by the scale at which the power spectrum peaks. At the end of inflation, the correlation scale L_{rh} is much smaller than the smoothing scale $L_\epsilon \sim 2\pi/(\epsilon aH)$ by a factor of ϵ/ξ .

- (3) The spectral index [Eq. (A14)] is given by the power of parameter ϵ in Eq. (3.38). Combining Eqs. (B19) and (3.31), we find $n_B = 3 - n$, as mentioned in Eq. (2.21).

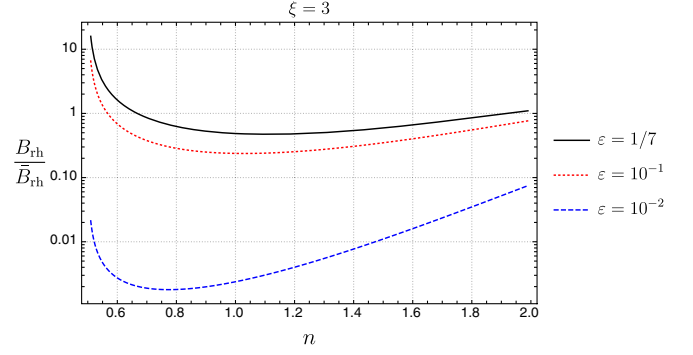


FIG. 2. The plot compares the amplitude of the magnetic field in Eq. (3.40) with its counterpart \bar{B}_{rh} in Eq. (2.18) obtained in the absence of stochastic effects. We have chosen $\xi = 3$ in order to avoid the backreaction problem. For $\epsilon \gtrsim \mathcal{O}(0.1)$, we have $B_{\text{rh}} \sim \mathcal{O}(\bar{B}_{\text{rh}})$, but for the consistency of the stochastic formalism, we require $\epsilon \ll 1$. As a result, we find a smaller intensity for the magnetic field in the presence of stochastic noises.

Therefore, the magnetic field intensity at the end of inflation is given by⁷

$$B_{\text{rh}} \simeq 5.3 \times 10^{55} \text{ G} \left(\frac{H}{M_{\text{Pl}}} \right)^2 \frac{\sqrt{\xi} \sinh(2\pi\xi) \Gamma(2n-1)}{2^n \sqrt{n+2}} e^{n_B}. \quad (3.40)$$

The above expression is the intensity of the magnetic field at the end of inflation when the stochastic noises are taken into account. As seen, B_{rh} depends on the Hubble parameter during inflation H , but it is also a function of n and ξ for a fixed value of ϵ . As we discussed before, the latter parameter controls the scale dependency of the magnetic field.

The expression (3.40) can be compared with its counterpart in Eq. (2.18), which is obtained in the absence of the stochastic effects. In Fig. 2, we have plotted the ratio between these two amplitudes for the same values of H and ξ in terms of n . The plot shows that in the stochastic approach, the intensity of the magnetic field at the end of inflation is smaller than what is obtained in the conventional method. This is because the stochastic process controlling the dynamics of the magnetic field is an OU process in which the stochastic force is balanced by the frictional drift force. Therefore, the tachyonic production of the gauge field is controlled by the stochastic noises, and the amplitude of the magnetic field becomes smaller than in conventional approaches where no stochastic effects are included.

The amplitude of H controls the energy scale of inflation, and it is usually estimated by the tensor-to-scalar ratio r_t . However, the tachyonic growth of the gauge field

⁷The unit conversion $1 \text{ GeV} = 3.8 \times 10^9 \text{ G}^{1/2}$ is used.

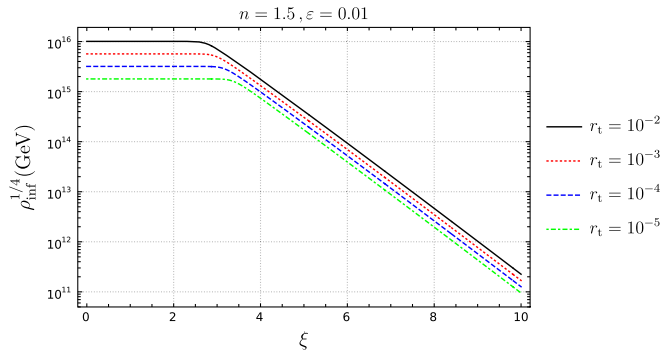


FIG. 3. Inflationary energy scale as a function of the parameter ξ with $n = 1.5$ and $\varepsilon = 0.01$ for various tensor-to-scalar ratios. For $\xi > 4$, the gauge field has the dominant contribution to r_t , and inflation has a low-energy scale, $\rho_{\text{inf}}^{1/4} \simeq 10^{-8} - 10^{-15} M_{\text{Pl}}$.

can source the tensor perturbations, so there is a contribution from the electromagnetic source to r_t as well. In Appendix E, we have estimated r_t in terms of the equilibrium amplitude of the electric field (for the interested range $1/2 < n < 2$) as a source for tensor perturbations. Based on the results from Appendix E, we have shown in Fig. 3 how the energy scale of inflation depends on the model parameters. Having the Hubble parameter during inflation [Eq. (E9)] at hand, one finds the final result for the intensity of the magnetic field at the end of inflation $B_{\text{rh}}(n, \xi, r_t)$. We comment that a very small value of $H/M_{\text{Pl}} \sim 10^{-20}$ has been advocated in Refs. [52,53] in order to generate the observationally required value of the primordial magnetic field. As we mentioned previously, this is because those studies allowed for $\xi \simeq 10-20$, while in our analysis, taking the backreaction and the stochastic effects all into account, we can go as far as $\xi \simeq 3$.

In order to evaluate the intensity and the correlation length of the magnetic field today, we need to study its time evolution after the end of inflation. In Appendix A, we have reviewed the cosmological evolution of the helical and nonhelical magnetic fields from the time of the end of inflation, B_{rh} , until today, B_0 . In the next section, we employ the results of Appendix A to estimate the amplitudes of the magnetic fields generated in the presence of the stochastic noises.

IV. PRESENT MAGNETIC FIELDS

A successful primordial magnetogenesis mechanism should generate an initial magnetic seed with sufficient strength. Having Eq. (3.40) as our primordial seed at the end of inflation, we study its evolution until today using the relations presented in Appendix A. The seed field could be amplified by either astrophysical or primordial processes to produce the observed magnetic field today and to satisfy the IGMF and GMF observational constraints, as pointed out in the Introduction. In what follows, we will present these constraints with more details and then investigate the

parameters of the model with which the constraints relating to GMFs and/or IGMFs could be satisfied.

A. Observational constraints

We are interested in two classes of observations, GMF and IGMF, that may hint towards the primordial origin of the cosmological magnetic fields and could be sourced by the seed field [Eq. (3.40)]. The former corresponds to the galactic scale, while the latter deals with the extragalactic scale. Although the astrophysical mechanisms of generation, such as the Biermann battery or the ejection of magnetic fields from stars, have been assumed as possible seeds for the galactic dynamo and GMFs, it would be difficult to provide fields that can account for the lower bound of IGMFs because the bound applies in the absence of matter structure or ionized plasma [29]. Therefore, IGMF observations can be considered as a strong hint on the necessity of primordial magnetic seeds. The details of the observations are as follows.

(1) GMFs:

Using a number of techniques, magnetic fields of the order of

$$B_{\text{GMF}} \sim \mu\text{G} \quad (4.1)$$

are observed in galaxies which are tens of Kpc in scale. For example, our galaxy is permeated by a magnetic field with strength $3-4 \mu\text{G}$ [76], while magnetic fields with similar magnitudes (with strength $1-10 \mu\text{G}$) have also been observed in clusters of galaxies on scales of up to $\sim 0.1 \text{ Mpc}$ [77,78]. A primordial magnetic seed with a minimal amplitude $\sim n\text{G}$ can be amplified to the desired strength by simple adiabatic contraction, while the seeds with much smaller amplitudes must be amplified by stronger processes—e.g., the galactic dynamo mechanism.

The dynamo mechanism transfers the kinetic energy of fluid into magnetic energy. More precisely, the coarse-grained hydrodynamics fluctuations can amplify a weak seed of a magnetic field by providing the electromotive forces.⁸ For instance, a field of order 10^{-30} G at 10 kpc is sufficient to initiate the dynamo process [79]. On the other hand, it is claimed in Ref. [8] that a seed field of 10^{-23} G at $\sim \text{Mpc}$ is needed to initiate the dynamo mechanism. To estimate the intensity of a magnetic field at the $\sim \text{Mpc}$ scale via an inverse cascade process, we follow Refs. [53,80], in which a seed field in the range of

⁸For comprehensive reviews of magnetic fields in the early Universe, see for instance Refs. [8,25].

$$10^{-23} \text{ G} \lesssim B_{\text{seed}} \lesssim 10^{-21} \text{ G} \quad (4.2)$$

at the Mpc scale is required to explain the observed μG magnetic fields in galaxies via the dynamo mechanism. It must be noted that due to the complicated galactic magnetohydrodynamics process, there is a large uncertainty on the ranges given in Eq. (4.2). Moreover, the observation of magnetic fields with the same order in protogalactic clouds at high redshift is against the validity of galactic dynamo mechanism [81,82]. However, it is usually assumed that the observed GMF is the end product of this mechanism [80]. Therefore, we consider Eq. (4.2) as a reference value for the seed amplitude.

(2) IGMFs:

The IGMF constraint is based on the nonobservation of GeV photons from TeV blazars and active galactic nuclei [28]. IGMFs lead to a lower bound on the intensity of magnetic fields in the intergalactic medium with a correlation length of 1 Mpc or more [83]. This bound is strengthened for the smaller correlation length. Several observations [5,84–90] have constrained the strength of the cosmological magnetic fields in this class to be [91,92]

$$B_{\text{IGMF}} \gtrsim 10^{-16} \text{ G} \times \begin{cases} 1, & L_{\text{B}} \gtrsim 1 \text{ Mpc} \\ \sqrt{\frac{1 \text{ Mpc}}{L_{\text{B}}}}, & L_{\text{B}} \lesssim 1 \text{ Mpc} \end{cases} \quad (4.3)$$

In addition, there is an upper bound $B_{\text{IGMF}} \lesssim 10^{-9} \text{ G}$ coming from the CMB data. There are two points here that must be mentioned: First, the above observation puts a constraint not only on the intensity of the magnetic field but also on its correlation length. Second, the lower bound 10^{-16} G on Mpc scales is not very rigid, and it could take a wide range with a width of 3 orders of magnitude, $10^{-15} - 10^{-18} \text{ G}$, depending on the details of cascade emission and its time delay [31,83].

The large correlation length involved in the bounds (4.3) and (4.2) may hint towards the primordial origin of the cosmological magnetic fields. We are interested in the parameter space in which the primordial magnetic fields [Eq. (3.40)] satisfy the lower bound in IGMFs [Eq. (4.3)] and provides the seed [Eq. (4.2)] for GMFs, assuming the galactic dynamo mechanism as the amplification mechanism.

In order to study the cosmological evolution of the primordial magnetic fields, we should consider the flux conservation as well as the helicity conservation. The relations between the present amplitude of the magnetic field B_0 and the reheating value B_{rh} for the flux and helicity conservations are given in Eqs. (A18) and (A22), respectively. Depending on the characteristics of the magnetic field produced during inflation, as well as the characteristics of the environment through which it passes, one of the

two conservation laws could be at work. The modes that exit the horizon during inflation at early times will be less affected by the plasma turbulence when they reenter the horizon after recombination. Therefore, the flux conservation is a good approximation for studying their evolution. On the other hand, the modes that exit the horizon at later times will encounter the turbulent plasma at the reentry time. Hence, their flux is not conserved, so we study their evolution via helicity conservation. More precisely, there exists a special scale k_{diss} at which the Reynolds number of plasma is at the order of unity. Modes with $k > k_{\text{diss}}$ ($k < k_{\text{diss}}$) come across the plasma at the turbulent (viscous) regime, so in order to study their subsequent evolution, we can easily consider helicity (flux) conservation. In the following, we use the superscripts F and H to denote the present magnetic fields B_0^F and B_0^H , which are evolved via the flux and helicity conservations, respectively.

For a small value of ξ , the generated magnetic field is nonhelical, so one can track the evolution of the magnetic field by imposing the flux conservation. For helical fields, however, the situation is different. It is well studied that during the radiation-dominated epoch, the helical magnetic fields undergo the inverse cascade process [51,93]. During this process, the intensity of the magnetic field decreases in the comoving frame, and its correlation scale increases while the power is transferred from small to large scales. Furthermore, it displays a property of self-similarity—i.e., the magnetic spectral index at scales larger than the correlation scale remains unchanged.

B. Flux conservation

For $\xi \lesssim 1$, the magnetic field is basically nonhelical. Neglecting the resistivity and the turbulence of the primordial plasma, one can estimate the strength of the

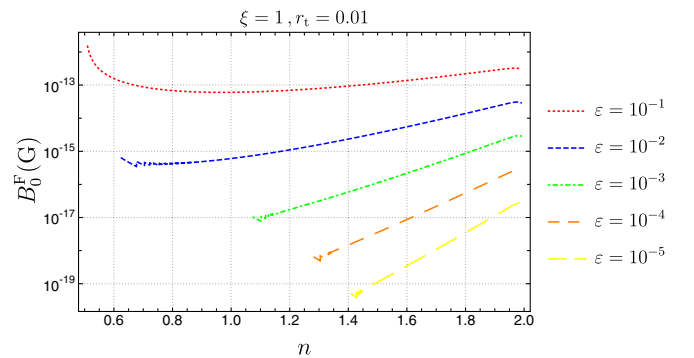


FIG. 4. Present value of magnetic field at the Mpc scale in terms of parameter n according to Eq. (4.4) for $\xi = 1$, in which flux conservation is assumed. As seen, the generated magnetic field easily satisfies the observational IGMF bound [Eq. (4.3)], but not the GMF bound via the galactic dynamo mechanism. One may consider a process weaker than the dynamo mechanism to amplify the intensity to the order of 10^{-15} G to μG observed in galaxies.

magnetic fields at the present time. Assuming radiation-like dilution for the electromagnetic energy density and also an instant reheating scenario after the end of inflation⁹ leads to

$$B_0^F \simeq 1.7 \times 10^{-6} \text{ G} \left(\frac{H}{M_{\text{Pl}}} \right) \frac{\sqrt{\xi} \sinh(2\pi\xi) \Gamma(2n-1)}{2^n \sqrt{n+2}} \epsilon^{n_B}, \quad (4.4)$$

in which we have inserted Eq. (3.40) into Eq. (A18). Using the relation (E9) for the Hubble parameter, which represents the energy scale of inflation, the behavior of the present amplitude of the magnetic field B_0^F in terms of the parameters of the model, n, ξ, r_t , is obtained. The result is plotted in Fig. 4. The energy scale of inflation is also plotted in Fig. 3. We see that taking into account the stochastic noises, an acceptable amplitude for the present magnetic field is generated [54] with a high-energy scale of inflation.

C. Helicity conservation

For $\xi > 1$, the generated magnetic field at the end of inflation is maximally helical.¹⁰ After inflation, the thermal cosmic plasma contains many relativistic charged particles and can be treated as an MHD plasma. In this limit, the electric field is damped away, and the magnetic field undergoes an inverse cascade due to helicity conservation. Therefore, the discussion presented in Appendix B is relevant.

Inserting Eq. (3.40) into Eq. (A22), the intensity of the present magnetic field at the correlation scale $L_0^H = 10^8 \text{ Mpc}(B_0^H/\text{G})$ is obtained to be

$$B_0^H = 5 \times 10^{-16} \text{ G} \left(\frac{H}{M_{\text{Pl}}} \right)^{1/2} \left(\frac{\Gamma^2(2n-1)}{2^{2n+1}(n+2)} e^{2\pi\xi} \epsilon^{2n_B} \right)^{1/3}. \quad (4.5)$$

Since we are interested in Mpc scales, the correction arising from the scale dependence must be taken into account via the relation (A19). Upon doing so, the amplitude of the magnetic field at Mpc scales is obtained to be

$$B_{\text{Mpc}} = B_0^H \left(\frac{L_0^H}{\text{Mpc}} \right)^{n_B}. \quad (4.6)$$

In Fig. 5, we have presented B_{Mpc} in terms of n and found that the maximum value of the intensity of the magnetic field is not stronger than 10^{-28} G , which is too small to be considered as a seed field [Eq. (4.2)] to initiate the galactic dynamo and explain the GMF constraints. One

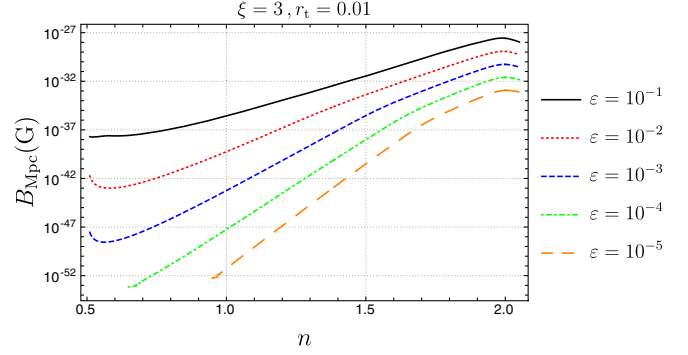


FIG. 5. Present value of magnetic field at the Mpc scale in terms of parameter n according to Eq. (4.6), in which helicity conservation is assumed for $\xi = 3$. As seen, the primordial seed field [Eq. (3.40)] is not strong enough to provide the initial seed needed in Eq. (4.2) for the dynamo mechanism. One will need a process stronger than the dynamo mechanism to amplify the intensity to the order of 10^{-30} G to μG observed in galaxies for the parameter space $n \lesssim 2$.

would need a stronger process in order to amplify this small seed value to the desired amplitude.¹¹

To investigate the IGMF constraint, we follow the method used in Refs. [32,52]. The magnetic fields with minimal amplitude of the order of 10^{-18} G and correlation length $L_0^H \gtrsim D_e$ can explain the nonobservation of GeV gamma-ray cascades around blazars in the intergalactic medium (IGM) [28,31,83], in which D_e is the electron/positron energy loss length for inverse Compton scattering. The correlation length of our setup is typically in the range $L_0^H \simeq 10^{-3} - 10^{-9} \text{ pc}$, which is much smaller than $D_e \simeq 80 \text{ Kpc}$. Taking into account the correction arising from the scale dependence for $n_B > 1/2$ (equivalent to $n < 5/2$), the constraint [Eq. (4.3)] for $L_0^H \ll D_e$ is translated into the following upper bound [32]:

$$B_0^H \gtrsim B_{\text{obs}} \sqrt{\frac{D_e}{L_0^H}} \sqrt{\frac{10n_B - 5}{n_B}}, \quad (4.7)$$

where $B_{\text{obs}} = 10^{-18} - 10^{-16} \text{ G}$.

The above constraint will need a large value of ξ , say $\xi \sim 10-20$. However, this large value of ξ is not allowed, since it induces large backreactions on the scalar field dynamics. In Fig. 6, we have shown the allowed regions in parameter space $\xi - n$ in which the backreaction problem is bypassed and the constraint of Eq. (4.7) is satisfied. As seen, there is no overlapping region, and the primordial seed fields [Eq. (3.40)] cannot satisfy the IGMF constraint [Eq. (4.3)].

⁹See Ref. [94] for a different discussion.

¹⁰For a different mechanism of helical magnetogenesis, see Ref. [95].

¹¹It should be noted that we have considered the strong coupling regime, in which $0 < n < \frac{1}{2}$, as well, and the result for the magnetic field did not change much from Fig. 5.

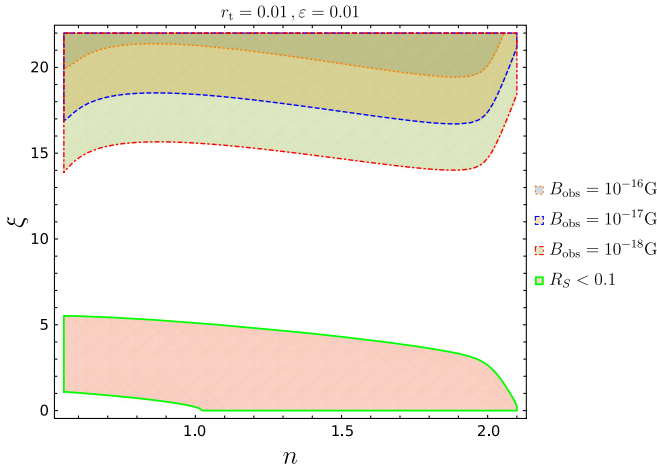


FIG. 6. The allowed region with small backreaction $R_S < 1$ [Eq. (3.25)] is confined in the lower bounded area (red area). The parameter space where the IGMF constraint [Eq. (4.7)] is satisfied is confined in the upper parts bounded by different curves (red, blue, and orange). There is no overlapping area, which means that the model with the maximally helical seeds cannot satisfy the IGMF constraint.

V. CONCLUSION

In this paper, we have revisited the mechanism of magnetogenesis in the $I^2F\bar{F}$ inflationary model by taking into account the stochastic effects of the electromagnetic field perturbations. We have derived the associated Langevin equations for the electric and magnetic fields and have calculated their two-point correlations. The corresponding Langevin equations are in the form of Ornstein-Uhlenbeck stochastic differential equations with a negative drift coefficient. We have shown that both the electric and magnetic fields settle into equilibrium states very quickly, with the strengths given by Eqs. (3.33) and (3.31), respectively.

We also checked the backreaction constraint and found that the instability parameter has an upper bound $\xi \lesssim 3$ in order for the backreaction of electromagnetic fields on the dynamics of the inflaton field to be under control. This bound is consistent with the results of Refs. [66,68]. In addition, the backreaction effects become stronger when we use a test field instead of inflatons, because the slow-roll parameter associated with the test field is smaller than that of the inflaton field.

The results show that the stochastic effects cause the amplitude of the magnetic field at the end of inflation to be smaller than what is obtained in the conventional method by at least 2 orders of magnitude; see Fig. 2. The stochastic forces tame the tachyonic growth of IR modes, which are described by an OU-type stochastic differential equation. The process settles the fields into equilibrium states and decreases their exponential growths.

The setup with $\xi > 1$ produces magnetic fields with a net helicity. Therefore, the helicity conservation must be

considered for the evolution of the magnetic field from the end of inflation until today. But, as mentioned above, the backreaction constraint requires $\xi \lesssim 3$, so the tachyonic growth of the electromagnetic perturbations is limited and the observational constraints of Eqs. (4.2) and (4.3) are not satisfied. Therefore, in the parameter space where the backreaction is under control, the model is not able to provide a chiral primordial seed for GMFs and IGMFs. Furthermore, as shown in Fig. 3, with $\xi \lesssim 3$, the energy scale of inflation can be as high as $10^{-3} - 10^{-4} M_{\text{Pl}}$. These results are in contrast with the results of Refs. [52,53], in which it is claimed that the model with $\xi \sim \mathcal{O}(10)$ is able not only to account for the IGMF observations, but also to initiate the galactic dynamo by providing the seed field in the range of Eq. (4.2) while inflation is happening at a low-energy scale.

On the other hand, for $\xi < 1$, the generated magnetic field is not helical, and one can simply study the evolution of the magnetic field via flux conservation. This yields the present magnetic field with the amplitude $B_0^f \simeq 10^{-13}$ G on Mpc for $n \simeq 2$, which is well suitable into the IGMF bound [Eq. (4.3)]. The generated seed field is too strong for the galactic dynamo mechanism, but one can consider another weaker process—e.g., adiabatic contraction—to amplify these magnetic fields to provide the intensity of the order of $\sim \mu\text{G}$ on galactic scales.

ACKNOWLEDGMENTS

H. F. and A. T. would like to thank the ‘‘Saramadan’’ federation of Iran for their partial support.

APPENDIX A: COSMOLOGICAL EVOLUTION OF MAGNETIC FIELDS

In this Appendix, we briefly review the evolution of cosmological magnetic fields in an expanding Universe filled with and without the cosmic plasma. We refer the reader to Refs. [7,51] for detailed and critical reviews of the literature on the subject.

Due to the homogeneity and isotropy of the Universe, it is more convenient to study the properties of its magnetic field in terms of its Fourier components,

$$\mathbf{B}(\mathbf{k}, t) = \int d^3x \mathbf{B}(\mathbf{x}, t) e^{i\mathbf{k}\cdot\mathbf{x}}. \quad (\text{A1})$$

Using Eqs. (2.5) and (2.12), we obtain

$$B_i(\mathbf{k}, \tau) = \sum_{\lambda=\pm} e_i^\lambda(\mathbf{k}) (B_\lambda(k, \tau) a_{\mathbf{k},\lambda} + B_\lambda^*(k, \tau) a_{-\mathbf{k},\lambda}^\dagger), \quad (\text{A2})$$

where $k = |\mathbf{k}|$ and $B_\lambda(k, \tau) = \lambda k v_{k,\lambda}(\tau)$. The spatial structure of magnetic fields is statistically the same at any location in the Universe, which implies that the expectation

values of the magnetic fields only depend on \mathbf{k} , δ_{ij} , and ϵ_{ijk} , as well as combinations of these.

The two-point function of the Fourier components of the magnetic field, which is a divergence-free vector field, in the comoving coordinate, can be written as

$$\begin{aligned} & \langle B_i(\mathbf{k}, \tau) B_j^*(\mathbf{q}, \tau) \rangle \\ &= (2\pi)^3 \frac{\delta(\mathbf{k} - \mathbf{q})}{k^3} ((\delta_{ij} - \hat{k}_i \hat{k}_j) \mathcal{P}_B(k, \tau) - i \epsilon_{ijl} \hat{k}_l \mathcal{H}_B(k, \tau)), \end{aligned} \quad (\text{A3})$$

where $\hat{\mathbf{k}} = \mathbf{k}/k$, and the bracket $\langle \rangle$ denotes an ensemble average.

The symmetric and antisymmetric parts of the above correlation are denoted by \mathcal{P}_B and \mathcal{H}_B , respectively—i.e.,

$$\sum_{\lambda=\pm} \langle B_\lambda(\mathbf{k}, \tau) B_\lambda^*(\mathbf{q}, \tau) \rangle = (2\pi)^3 \frac{\delta(\mathbf{k} - \mathbf{q})}{k^3} \mathcal{P}_B(k, \tau), \quad (\text{A4})$$

$$\sum_{\lambda=\pm} \lambda \langle B_\lambda(\mathbf{k}, \tau) B_\lambda^*(\mathbf{q}, \tau) \rangle = (2\pi)^3 \frac{\delta(\mathbf{k} - \mathbf{q})}{k^3} \mathcal{H}_B(k, \tau). \quad (\text{A5})$$

The symmetric part of the spectrum determines the energy density,

$$\rho_B(\tau) \equiv \frac{1}{2\pi^2} \int d \ln k \mathcal{P}_B(k, \tau). \quad (\text{A6})$$

Therefore, $\mathcal{P}_B(k, \tau)$ is related to the magnetic energy density per logarithmic wave number via

$$\mathcal{P}_B(k, \tau) = 2\pi^2 \frac{d\rho_B(k, \tau)}{d \ln k}. \quad (\text{A7})$$

The magnetic helicity is defined as

$$H(V, \tau) = \int_V d^3x \langle \mathbf{A}(\mathbf{x}, \tau) \cdot \mathbf{B}(\mathbf{x}, \tau) \rangle, \quad (\text{A8})$$

where V is a volume through the boundary of which no magnetic field lines cross. For the gauge in which the 3D vector potential \mathbf{A} is transverse, we define the magnetic helicity density as

$$\mathfrak{h}(\tau) \equiv \langle \mathbf{A}(\mathbf{x}, \tau) \cdot \mathbf{B}(\mathbf{x}, \tau) \rangle = \frac{1}{2\pi^2} \int d \ln k \mathcal{H}_B(k, \tau). \quad (\text{A9})$$

Hence, $\mathcal{H}_B(k, \tau)$ is related to the helicity density per logarithmic interval,

$$\mathcal{H}_B(k, \tau) = 2\pi^2 \frac{d\mathfrak{h}(\tau)}{d \ln k}. \quad (\text{A10})$$

It is convenient to assign two characteristic properties to the magnetic fields. First, the characteristic correlation

length L , which is sometimes called the correlation scale, is defined via

$$L \equiv \frac{\int d \ln k \frac{(2\pi/k) \mathcal{P}_B(k)}{\mathcal{P}_B(k)}}{\int d \ln k \mathcal{P}_B(k)}, \quad (\text{A11})$$

which is a measure of the scale containing most of the magnetic energy.

Second, the scale-averaged magnetic strength is given by

$$B \equiv \sqrt{2\rho_B}, \quad (\text{A12})$$

while the characteristic magnetic field strength at scale $\ell = 2\pi/k$ is defined as

$$B_\ell \equiv \sqrt{2 \frac{d\rho_B}{d \ln k} \Big|_{k=2\pi/\ell}} = \frac{\sqrt{\mathcal{P}_B(k)}}{\pi} \Big|_{k=2\pi/\ell}. \quad (\text{A13})$$

In addition, the magnetic spectral index on large scales is defined as

$$n_B \equiv \frac{1}{2} \frac{d \ln \mathcal{P}_B(k)}{d \ln k}. \quad (\text{A14})$$

For example, in the model $I(\tau) F_{\mu\nu} F^{\mu\nu}$ with $I(\tau) \propto \tau^n$, the magnetic field spectral index is given by $n_B = \frac{5}{2} - |n - \frac{1}{2}|$ so that the cases with $n = 3$ and $n = -2$ lead to scale-invariant magnetic spectra.

To study the expected relic magnetic field, which might survive until the present epoch, we must have enough knowledge about the initial spectrum of the magnetic field generated during inflation—i.e., \mathcal{P}_B and \mathcal{H}_B —and know their evolution well after inflation and the reheating phase.

In the first approximation, the conductivity of the Universe, which is very high after reheating, must be considered. Therefore, any electric fields produced during inflation will be damped very rapidly after inflation while the magnetic field is frozen. This is why we consider magnetogenesis models prior to reheating. The electric conductivity converts the generated electromagnetic modes into a frozen magnetic field which obeys adiabatic dilution—i.e., the magnetic power spectrum decays as $\mathcal{P}_B \propto a^{-4}$ after the mode function is frozen due to electric conductivity.

A better approximation is to consider a plasma environment instead of an electrically conductive medium. Due to the presence of many relativistic charged particles after inflation, the thermal cosmic plasma can be treated as a magnetohydrodynamic (MHD) plasma. An important characteristic of the fluid flow is given by its local kinetic Reynolds number, denoted by R_ℓ . The Reynolds number is a measure of the relative importance of fluid dissipative terms in the Euler equations of MHD fluid. In general, in the MHD limit, the electric fields are damped away, while the magnetic fields' evolution must be studied in two

different regimes: the turbulent regime, when $R_e \gg 1$, and the viscous regime, when $R_e \ll 1$. In the former regime, the magnetic field is damped on small scales, which leads to a maximally helical field—i.e., one of the polarization modes vanishes [51]. Therefore, the magnetic fields undergo an inverse cascade due to *helicity conservation* [80]. This effect is active as long as $R_e > 1$ on the scale under consideration. Therefore, the fluid is turbulent in the regime in which the decay rate of the total energy only depends on the flow properties on the integral scale and is independent of dissipative terms. This regime is applicable well before the neutrino decoupling and recombination. After the end of the turbulent phase, magnetic fields are damped on small scales by viscosity and evolve by *flux conservation*, so that $B \propto a^{-2}$ on large scales.

In the viscous regime, the decay of magnetic energy depends on the magnitude of viscosities. This regime describes the state of the cosmic plasma, before recombination, on scales smaller than the damping scale k_{diss} at which R_e becomes of order unity. Both the turbulent motion of the fluid and the magnetic field are damped exponentially by viscosity. Furthermore, there is the effect of ambipolar diffusion after recombination, when the Universe is a weakly ionized fluid. This diffusion is due to the ion-neutral mixture in the tightly coupled regime, which inserts an additional dissipative term in the MHD equations. We refer the reader to Refs. [7,51] for more details about the general features of the evolution of magnetized fluids, such as the decay of energy density, as well as the growth of magnetic field coherence length, in the turbulent and viscous regimes.

In what follows, we will study the evolution of the magnetic fields from the end of inflation (reheating) till the present time in terms of two different assumptions: flux conservation ($\rho_B \propto B^2 = \text{const.}$) and helicity conservation ($\mathfrak{h} \propto B^2 L = \text{const.}$). For the expanding Universe, these two conservation laws lead to $B^2 \propto a^{-4}$ and $B^2 L \propto a^{-3}$, respectively.

1. Flux conservation

In order to estimate the strength of the magnetic fields at the present time, we assume radiation-like dilution for the electromagnetic energy density and neglect the high conductivity and turbulence of the primordial plasma with an instant reheating scenario (see Ref. [94] for a controversial discussion). Due to the flux conservation, the amplitude of the magnetic field at the present time, denoted by B_0 , is given by

$$B_0 = \left(\frac{a_{\text{rh}}}{a_0}\right)^2 B_{\text{rh}}, \quad (\text{A15})$$

where the amplitude of the magnetic field at the end of inflation is denoted by B_{rh} , and a_{rh} and a_0 are the values of the scale factor at the end of inflation and at present,

respectively. To simplify the situation further, we assume that the Universe was radiation dominated throughout its history with a reasonable accuracy. Then, we have

$$\frac{a_0}{a_{\text{rh}}} = \left(\frac{g_{\text{rh}}^*}{g_0^*}\right)^{1/3} \frac{T_{\text{rh}}}{T_0}, \quad (\text{A16})$$

in which g_0^* and g_{rh}^* are the effective numbers of relativistic degrees of freedom at the present time and at the time of reheating, respectively. Moreover, an instant reheating scenario allows us to express T_{rh} in terms of the Hubble rate at the end of inflation H :

$$T_{\text{rh}} \simeq 1.5 \times 10^{31} \text{ K} \left(\frac{g_{\text{rh}}^*}{106.75}\right)^{-1/4} \left(\frac{H}{M_{\text{Pl}}}\right)^{1/2}. \quad (\text{A17})$$

Using these relations, the amplitude of the observed magnetic field at the present time is given by

$$B_0 \simeq 3.2 \times 10^{-62} \left(\frac{H}{M_{\text{Pl}}}\right)^{-1} B_{\text{rh}}, \quad (\text{A18})$$

where we have set $g_0^* = 3.36$ and $g_{\text{rh}}^* = 106.75$.

2. Helicity conservation

The evolution of B and L during the postinflationary epoch undergoes several different phases: turbulent, viscous, and free-streaming [7,51]. Not only do the initial values of the intensity and the correlation scale determine what phase the Universe is in, but also the particle species with the longest mean free path (neutrinos, followed by photons after neutrino decoupling) have significant effects on the evolution of the magnetic energy via the temperature of the kinetic viscosity of the plasma.

It is well known that in the turbulent fluid with nonvanishing helicity, the helical magnetic field undergoes a process known as inverse cascade during the radiation-dominated epoch. Considering this process, the comoving L increases and its comoving intensity B decreases. The power is transferred from small scales to large scales, while the magnetic spectrum at scales larger than L —i.e., $\ell > L$ —maintains its spectral index unchanged. Consequently, the amplitude of the magnetic field on large scales is given by

$$B_{\ell > L} = B \left(\frac{L}{\ell}\right)^{n_B}, \quad (\text{A19})$$

displaying a property of self-similarity [51]. It must be noted that the inverse cascade is not effective in the case of a (nearly) scale-invariant spectrum even for a fully helical magnetic field [96].

Taking into account high conductivity along with the turbulence of the primordial plasma, the magnetic fields evolve while conserving (comoving) magnetic helicity density (instead of magnetic flux) via the inverse cascade

process. Therefore, in an expanding Universe, we have

$$B_0^2 L_0 = \left(\frac{a_{\text{rh}}}{a_0}\right)^3 B_{\text{rh}}^2 L_{\text{rh}}, \quad (\text{A20})$$

where L_{rh} and L_0 are the correlation scale at the end of inflation and at the present time, respectively. The above relation must be considered along with a second relation in order to determine the present values of the magnetic intensity and its correlation scale. Reference [51] demonstrated that for a large set of initial conditions, the values of B and L at recombination are linked by the relation $B \simeq L H_{\text{rec}} \rho^{1/2}$, where H_{rec} is the Hubble parameter at recombination and ρ is the energy density of the fluid particles that couple to the magnetic field. Evolving this relation until today, under the condition that their comoving values stay constant, we find a very general relation [7,51]

$$B_0 \simeq 10^{-8} \text{ G} \left(\frac{L_0}{\text{Mpc}}\right). \quad (\text{A21})$$

The relations (A20) and (A21) are a consequence of the inverse cascade of the helical field associated with self-similar evolution.

One can determine the current values of the magnetic intensity and the correlation scale by combining Eqs. (A20) and (A21) to obtain

$$B_0 = 10^{-8} \text{ G} \left(\frac{B_{\text{rh}}}{10^{-8} \text{ G}}\right)^{2/3} \left(\frac{L_{\text{rh}}}{\text{Mpc}}\right)^{1/3} \left(\frac{a_{\text{rh}}}{a_0}\right), \quad (\text{A22})$$

$$L_0 = \left(\frac{B_{\text{rh}}}{10^{-8} \text{ G}}\right)^{2/3} \left(\frac{L_{\text{rh}}}{\text{Mpc}}\right)^{1/3} \left(\frac{a_{\text{rh}}}{a_0}\right) \text{ Mpc}. \quad (\text{A23})$$

Using Eqs. (A16) and (A17), the magnetic field intensity and the correlation scales can be obtained in terms of the Hubble rate at the end of inflation and other parameters of the model.

APPENDIX B: NOISE CORRELATIONS FOR THE HELICAL EM FIELDS

In this Appendix, we derive the explicit forms of the quantum noises arising from the short modes of electromagnetic fields. For the nonhelical electromagnetic fields, the corresponding results can be found in Refs. [54,63,64].

Expanding Eq. (3.7) in terms of the creation and annihilation operators $a_{\mathbf{k}}$ and $a_{\mathbf{k}}^\dagger$, we find

$$\begin{aligned} \hat{\sigma}_i^X(\mathbf{x}, t) = & -\frac{dk_c}{dt} \sum_{\lambda} \int \frac{d^3 k}{(2\pi)^3} \delta(k - k_c) \\ & \times e_i^\lambda(\mathbf{k}) (X_{k,\lambda}(t) a_{\mathbf{k},\lambda} + X_{k,\lambda}^*(t) a_{-\mathbf{k},\lambda}^\dagger) e^{i\mathbf{k}\cdot\mathbf{x}}, \quad (\text{B1}) \end{aligned}$$

where $k_c \equiv \epsilon a(t)H$. Without loss of generality, we assume $\mathbf{x} = r\hat{z}$ and consider the wave number $\hat{\mathbf{k}}$ and the polarization vectors $\mathbf{e}_\lambda(\hat{\mathbf{k}})$ as

$$\hat{\mathbf{k}} = (\sin\theta \cos\phi, \sin\theta \sin\phi, \cos\theta), \quad (\text{B2})$$

$$\begin{aligned} \mathbf{e}_\lambda(\hat{\mathbf{k}}) = & \frac{1}{\sqrt{2}} (\cos\theta \cos\phi - i\lambda \sin\phi, \\ & \cos\theta \sin\phi + i\lambda \cos\phi, -\sin\theta) \quad (\text{B3}) \end{aligned}$$

in Cartesian coordinates. One can easily check that the above satisfies the orthogonality relations [Eq. (2.13)].

To calculate the correlation of the helical noises, we use the fact that for any λ -dependent function g_λ , one has

$$\sum_{\lambda=\pm} g_\lambda e_i^\lambda(\hat{\mathbf{k}}) e_j^{\lambda*}(\hat{\mathbf{k}}) = \frac{1}{2} \sum_{\lambda=\pm} g_\lambda (\delta_{ij} - \hat{k}_i \hat{k}_j + i\lambda f_{ij}(\theta, \phi)), \quad (\text{B4})$$

where f_{ij} is an antisymmetric matrix, $f_{ij} = -f_{ji}$, given by

$$\begin{aligned} f_{21}(\theta) = & \cos\theta, \quad f_{32}(\theta, \phi) = \sin\theta \cos\phi, \\ f_{13}(\theta, \phi) = & \sin\theta \sin\phi. \quad (\text{B5}) \end{aligned}$$

Using the relations

$$\begin{aligned} \int_{\Omega} d\Omega e^{ikr \cos\theta} &= \int_{\phi=0}^{2\pi} d\phi \int_0^\pi \sin\theta d\theta e^{ikr \cos\theta} \\ &= 4\pi \frac{\sin(kr)}{kr} \Big|_{r=0}^{r=0} = 4\pi, \quad (\text{B6}) \end{aligned}$$

$$\int_{\Omega} d\Omega e^{ikr \cos\theta} (\delta_{ij} - \hat{k}_i \hat{k}_j) = \frac{8\pi}{3} \delta_{ij} \frac{\sin(kr)}{kr} \Big|_{r=0}^{r=0} = \frac{8\pi}{3} \delta_{ij}, \quad (\text{B7})$$

$$\int_{\Omega} d\Omega e^{ikr \cos\theta} f_{ij} \Big|_{r=0}^{r=0} = 0, \quad (\text{B8})$$

one can find that

$$\begin{aligned} & \langle \hat{\sigma}_i^X(t_1, \mathbf{x}) \hat{\sigma}_j^X(t_2, \mathbf{x}) \rangle \\ &= \frac{1}{18\pi^2} \frac{dk_c^3}{dt} \sum_{\lambda} |X_\lambda(t_1, k_c)|^2 \delta_{ij} \delta(t_1 - t_2). \quad (\text{B9}) \end{aligned}$$

Using Eq. (2.15) as well as the definition of electric and magnetic fields [Eq. (2.5)], we find

$$\langle \hat{\sigma}_i^E(N_1), \hat{\sigma}_j^E(N_2) \rangle = \frac{H^2 2^{1-2n} \varepsilon^{4-2n} \Gamma(2n)^2}{3\pi^2 M_{\text{Pl}}^2 |\Gamma(n + i\xi)|^2} \cosh(\pi\xi) \delta_{ij} \delta(N_1 - N_2), \quad 0 < n < 2, \quad (\text{B10})$$

$$\langle \hat{\sigma}_i^B(N_1), \hat{\sigma}_j^B(N_2) \rangle = \frac{H^2 \varepsilon^5 (2\varepsilon)^{-2|n-\frac{1}{2}|} \Gamma(2|n-\frac{1}{2}|)^2}{3\pi^2 M_{\text{Pl}}^2 |\Gamma(\frac{1}{2} + |n-\frac{1}{2}| + i\xi)|^2} \cosh(\pi\xi) \delta_{ij} \delta(N_1 - N_2), \quad 0 < n \neq \frac{1}{2} < 2, \quad (\text{B11})$$

while for $n = 1/2$ we have

$$\langle \hat{\sigma}_i^B(N_1), \hat{\sigma}_j^B(N_2) \rangle = \frac{H^2 \varepsilon^5 \log^2(\varepsilon)}{3\pi^3 M_{\text{Pl}}^2} \cosh(\pi\xi) \delta_{ij} \delta(N_1 - N_2), \quad n = \frac{1}{2}. \quad (\text{B12})$$

1. Disappearance of the quantum nature of the noises

Here, we show that the quantum nature of noises disappears on large scales. To this end, we show that the following commutator goes to zero in this limit:

$$\frac{[\hat{\tau}_X, \hat{\sigma}_X]}{D_X^2} \rightarrow 0, \quad (\text{B13})$$

where $\hat{\tau}_X$ is the noise corresponding to the conjugate momentum of X , defined by

$$\hat{\tau}_X(\mathbf{x}, t) = -\frac{dk_c}{dt} \int \frac{d^3k}{(2\pi)^3} \delta(k - k_c) e^{i\mathbf{k}\cdot\mathbf{x}} \hat{X}_k. \quad (\text{B14})$$

If we show that the above relation holds, then it is logical to neglect the quantum nature of X on large scales, while keeping the effects of the classical noise of the X field in the analysis.

Using Eq. (2.15), as well as the definition of electric and magnetic fields [Eq. (2.5)], we obtain the following equations for the commutators of electromagnetic fields and their conjugate momentum:

$$[\hat{\sigma}_i^E(N_1), \hat{\tau}_j^E(N_2)] = -\frac{2iH^2 \xi \varepsilon^4 \sinh(2\pi\xi)}{3\pi^2 M_p^2} \delta_{ij} \delta(N_1 - N_2), \quad 0 < n < 2. \quad (\text{B15})$$

Comparing Eqs. (B10) and (B15), we see that the ratio of the amplitude of the commutator to the amplitude of the noise of the electric field is $\mathcal{O}(\varepsilon^{2n})$ and can be neglected in the range in which we are interested. This shows that as long as $\varepsilon \ll 1$, the noises can be treated classically. In the same manner, one can write the amplitude of the magnetic field and its commutator as follows:

$$[\hat{\sigma}_i^B(N_1), \hat{\tau}_j^B(N_2)] = -\frac{iH^2 \varepsilon^5 \cosh(2\pi\xi)}{3\pi^2 M_p^2} \delta_{ij} \delta(N_1 - N_2), \quad 0 < n < 2. \quad (\text{B16})$$

We see that the ratio of the commutator to the amplitude of the magnetic field is $\mathcal{O}(\varepsilon^{2|n-\frac{1}{2}|})$ when $n \neq \frac{1}{2}$ and $\mathcal{O}(\log^{-2}(\varepsilon))$ when $n = \frac{1}{2}$. Therefore, we conclude that one can neglect the quantum nature of the noises and treat them as classical noises.

With the above property and the disappearance of the quantum nature of the noises, one can express the quantum noises $\hat{\sigma}_X(N)$ in terms of the classical normalized white noise σ as

$$\hat{\sigma}_i^X(N) \equiv D_X \sigma_i(N), \quad (\text{B17})$$

where

$$\begin{aligned} \langle \sigma_i(N) \rangle &= 0, \\ \langle \sigma_i(N_1) \sigma_j(N_2) \rangle &= \delta_{ij} \delta(N_1 - N_2), \end{aligned} \quad (\text{B18})$$

and for $n \neq 1/2$, the amplitude D_X is given by

$$D_X \simeq \frac{\sqrt{2 \cosh(\pi\xi)} \Gamma(2n-1)}{\pi\sqrt{3} 2^n |\Gamma(n+i\xi)|} \frac{H}{M_{\text{Pl}}} \varepsilon^{2-n} \times \begin{cases} (2n-1), & X = E \\ \varepsilon, & X = B \end{cases}. \quad (\text{B19})$$

This amplitude approaches what is obtained in Refs. [54,64] when $\xi \rightarrow 0$ for nonhelical electromagnetic noises where the two transverse modes are the same.

APPENDIX C: DIAGONALIZATION

In this Appendix, we solve the coupled Langevin equations

$$\mathcal{B}' = -(2+n)\mathcal{B} + D_B \sigma(N), \quad (\text{C1})$$

$$\mathcal{E}' = -(2-n)\mathcal{E} + 2n\gamma\mathcal{B} + D_E \sigma(N). \quad (\text{C2})$$

A common way of handling these equations is to look for a change of coordinates or a change of variables that

simplifies the problem. We use the diagonal matrix method to solve the equations. Let us write Eqs. (3.15) and (3.16) in the following matrix form:

$$\begin{pmatrix} \mathcal{E}' \\ \mathcal{B}' \end{pmatrix} = C \begin{pmatrix} \mathcal{E} \\ \mathcal{B} \end{pmatrix} + \sigma(N) \begin{pmatrix} D_E \\ D_B \end{pmatrix}, \quad (\text{C3})$$

where C is the matrix of coefficients given by

$$C \equiv \begin{pmatrix} n-2 & 2n\gamma \\ 0 & -(2+n) \end{pmatrix}. \quad (\text{C4})$$

Having the matrix of coefficients at hand, one can easily write the basis transformation matrix as

$$P = \begin{pmatrix} -\gamma & 1 \\ 1 & 0 \end{pmatrix}, \quad (\text{C5})$$

which is obtained using the eigenvectors of C .

Now, according to the fact that any vector like V in the old basis changes as $\tilde{V} = P^{-1}V$ in the new basis, one can write Eq. (C3) as

$$\begin{pmatrix} \tilde{\mathcal{E}}' \\ \tilde{\mathcal{B}}' \end{pmatrix} = \tilde{C} \begin{pmatrix} \tilde{\mathcal{E}} \\ \tilde{\mathcal{B}} \end{pmatrix} + \sigma(N) \begin{pmatrix} D_B \\ D_E + \gamma D_B \end{pmatrix}, \quad (\text{C6})$$

where

$$\tilde{C} \equiv P^{-1}CP = \begin{pmatrix} -(2+n) & 0 \\ 0 & n-2 \end{pmatrix}, \quad (\text{C7})$$

and the tilde in the components denotes the changed vector. Then, in the new basis we obtain

$$\tilde{\mathcal{E}}' = -(2+n)\tilde{\mathcal{E}} + D_B\sigma(N), \quad (\text{C8})$$

$$\tilde{\mathcal{B}}' = -(2-n)\tilde{\mathcal{B}} + (D_E + \gamma D_B)\sigma(N). \quad (\text{C9})$$

Note that since the electric and magnetic fields originate from the same gauge field, the noises σ_B and σ_E are not independent—i.e., $\sigma_B + \sigma_E = (D_B + D_E)\sigma(N)$.¹² Then, we obtain two decoupled Langevin equations, which can be solved easily by the appropriate initial conditions, $\mathcal{B}(N=0) = \mathcal{B}_0$ and $\mathcal{E}(N=0) = \mathcal{E}_0$. More specifically, the solutions are given by

$$\begin{pmatrix} \tilde{\mathcal{E}}(N) \\ \tilde{\mathcal{B}}(N) \end{pmatrix} = \begin{pmatrix} \mathcal{B}_0 e^{-(n+2)N} + D_B \int_0^N e^{-(n+2)(N'-N)} \sigma(N') dN' \\ (\mathcal{E}_0 + \gamma \mathcal{B}_0) e^{(n-2)N} + (D_E + \gamma D_B) \int_0^N e^{-(n-2)(N'-N)} \sigma(N') dN' \end{pmatrix}. \quad (\text{C10})$$

Now, going back to the old basis by $\begin{pmatrix} \mathcal{E} \\ \mathcal{B} \end{pmatrix} = P \begin{pmatrix} \tilde{\mathcal{E}} \\ \tilde{\mathcal{B}} \end{pmatrix}$, we have

$$\mathcal{B}(N) = \mathcal{B}_0 e^{-(n+2)N} + D_B \int_0^N e^{-(n+2)(N'-N)} \sigma(N') dN', \quad (\text{C11})$$

$$\mathcal{E}(N) = e^{(n-2)N} (\mathcal{E}_0 + \gamma \mathcal{B}_0) - \gamma \mathcal{B}(N) + (D_E + \gamma D_B) \int_0^N e^{-(n-2)(N'-N)} \sigma(N') dN'. \quad (\text{C12})$$

APPENDIX D: PROBABILISTIC ANALYSIS

In this section, we use another approach to study the Langevin equation (3.15). Let us recast Eq. (3.15) into the following stochastic differential equation (SDE):

$$\frac{d\mathcal{B}_i(N)}{dN} = -\mu \mathcal{B}_i(N) + D_B \xi_i(N), \quad \mu \equiv n+2. \quad (\text{D1})$$

We are interested in the regime $\mu > 0$, so the above equation describes an Ornstein-Uhlenbeck (OU) process. Therefore, the field \mathcal{B}_i admits an equilibrium state with a

long-term mean and a bounded variance (mean-reverting process) due to the fact that the random force $D_B \xi_i$ balances the frictional drift force $-\mu \mathcal{B}_i$. To be more precise, an OU process is a stationary Gauss-Markov process, in which there is the tendency for the system to drift toward the mean value, with a greater attraction when the process is further away from the mean. For this process, the explicit dependence of the mean on the initial conditions is washed out over time, and the system can only be described by the drift μ and the diffusion D_B coefficients. In other words, the distribution of the random variable \mathcal{B}_i can be described by the normal distribution $\mathbb{N}(0, \frac{D_B^2}{2\mu})$ at $N = N_{\text{eq}}^B$. Formally, N_{eq}^B goes to infinity, but we can estimate the equilibrium time as when the relative difference of the field with its equilibrium

¹²Otherwise, we have $\sigma_B + \sigma_E = (D_B + D_E)^{1/2} \sigma(N)$.

value drops to a small value—say, 10^{-2} . With this approximation, we obtain Eq. (3.30).

Alternatively, the Fokker-Planck equation associated with the Langevin equation (D1) can be employed to describe the time evolution of the probability density function (PDF) of $\mathcal{B}_i(N)$. Consider $f_{\mathcal{B}_i}(x, N)$ as the PDF of the random variable \mathcal{B}_i . Then the associated Fokker-Planck equation is given by

$$\frac{\partial f_{\mathcal{B}_i}(x, N)}{\partial N} = -\mu \frac{\partial}{\partial x} (x f_{\mathcal{B}_i}(x, N)) + \frac{D_B^2}{2} \frac{\partial^2}{\partial x^2} f_{\mathcal{B}_i}(x, N). \quad (\text{D2})$$

Intuitively, one can think of $f_{\mathcal{B}_i}(x, N)dx$ as the probability of \mathcal{B}_i falling within the infinitesimal interval $[x, x + dx]$. Assuming a stationary probability distribution, $\partial f_{\mathcal{B}_i}^{\text{eq}}/\partial N = 0$, the equilibrium solution of Fokker-Planck Eq. (D2) is given by

$$f_{\mathcal{B}_i}^{\text{eq}}(x) = \sqrt{\frac{\mu}{\pi D_B^2}} \exp\left(-\frac{\mu}{D_B^2} x^2\right). \quad (\text{D3})$$

Using the above PDF for the components of the magnetic field \mathcal{B}_i , it is easy to obtain the PDF of its magnitude $\mathcal{B} \equiv (\sum_{i=1}^3 \mathcal{B}_i^2)^{1/2}$ as follows:

$$f_{\mathcal{B}}^{\text{eq}}(x) = 4\sqrt{\frac{\mu^3}{\pi D_B^6}} x^2 \exp\left(-\frac{\mu}{D_B^2} x^2\right). \quad (\text{D4})$$

This density function allows us to calculate the m th moment associated with \mathcal{B} as follows:

$$\begin{aligned} \langle \mathcal{B}^m \rangle_{\text{eq}} &= \int_0^\infty dx x^m f_{\mathcal{B}}^{\text{eq}}(x) \\ &= \frac{2}{\sqrt{\pi}} \left(\frac{D_B}{\sqrt{\mu}}\right)^m \Gamma\left(\frac{m+3}{2}\right), \end{aligned} \quad (\text{D5})$$

Moreover, these PDFs enable us to calculate the probability of having a given amplitude for the magnetic field in a given range. The desired range corresponds to the lower and upper bounds on cosmological magnetic fields as given in Eq. (4.3). Subsequently, these bounds are translated into the interval $\mathcal{B}_1 < \mathcal{B} < \mathcal{B}_2$. Therefore, one can calculate the probability of the generated magnetic field acquiring a value in the interval determined in Eq. (4.3), given by

$$\begin{aligned} P_{B_{\text{obs}}} &= \int_{\mathcal{B}_1}^{\mathcal{B}_2} dx f_{\mathcal{B}}^{\text{eq}}(x) \\ &= \text{Erf}(y_2) - \text{Erf}(y_1) - \frac{2}{\sqrt{\pi}} (y_2 e^{-y_2^2} - y_1 e^{-y_1^2}), \end{aligned} \quad (\text{D6})$$

in which $y_i \equiv \frac{\sqrt{\mu}}{D_B} \mathcal{B}_i$ and $i = 1, 2$. In fact, the above is the probability of generating the primordial magnetic field

consistent with the observational bound (4.3) by the model (2.3), $P_{B_{\text{obs}}}(n, \xi, \epsilon)$. The probabilistic interpretation based on the Fokker-Planck equation is a parallel approach to the mechanism of stochastic differential equations presented in Sec. IV.

It is interesting to obtain the stationary PDF of the electric field. One can write Eq. (3.18) as follows:

$$\begin{aligned} \mathcal{E}_i(N) + \gamma \mathcal{B}_i(N) \\ = (D_E + \gamma D_B) \int_0^N e^{-(n-2)(N'-N)} \sigma_i(N') dW(N'). \end{aligned} \quad (\text{D7})$$

As can be seen, the stochastic variable $\mathcal{E}_i(N) + \gamma \mathcal{B}_i(N)$ satisfies a Gaussian PDF. As $\gamma \mathcal{B}_i$ is a Gaussian variable, one can easily see that $(\mathcal{E}_i(N) + \gamma \mathcal{B}_i(N)) - \gamma \mathcal{B}_i(N)$ is a Gaussian as well. Therefore, by the mean and variance of electric field at the equilibrium state, one finds

$$f_{\mathcal{E}_i}^{\text{eq}}(x) = \sqrt{\frac{1}{\pi \langle \mathcal{E}_i^2 \rangle_{\text{eq}}}} \exp\left(-\frac{x^2}{\langle \mathcal{E}_i^2 \rangle_{\text{eq}}}\right), \quad (\text{D8})$$

where $\langle \mathcal{E}_i^2 \rangle_{\text{eq}}$ is given by Eq. (3.33).

APPENDIX E: GRAVITATIONAL WAVES INDUCED BY GAUGE FIELDS AND THE ENERGY SCALE OF INFLATION

The gauge fields are the additional sources of tensor perturbations, besides the vacuum ones. Which contribution is the dominant one depends directly on the model parameter. For $\xi \sim \mathcal{O}(10)$, where the tachyonic enhancement of the gauge field is significant, the gravitational wave signal actively sourced by the gauge field is more significant. In this Appendix, we study the production of gravitational waves induced by the electromagnetic modes.

Let us turn on the tensor perturbations of the metric (2.4) via

$$ds^2 = a^2(\tau) [-d\tau^2 + (\delta_{ij} + h_{ij}) dx^i dx^j], \quad (\text{E1})$$

in which $h_{ij}(t, \mathbf{x})$ is the transverse-traceless (TT) tensor perturbation ($\partial_i h^{ij} = 0 = h^i_i$). The quadratic expansion of the action (2.3) for tensor part leads to [97,98]

$$\begin{aligned} S_t^{(2)} &= \frac{M_{\text{Pl}}^2}{8} \int d^3x d\tau a^2 \left[h'_{ij}{}^2 - (\partial_k h_{ij})^2 - \frac{4a^2}{M_{\text{Pl}}^2} h_{ij} S_{ij} \right], \\ S_{ij} &= E_i E_j + B_i B_j. \end{aligned} \quad (\text{E2})$$

Therefore, the equation of motion for the tensor modes is given by

$$h''_{ij} + 2\mathcal{H}h'_{ij} - \nabla^2 h_{ij} = -\frac{2a^2}{M_{\text{Pl}}^2} S_{ij}, \quad (\text{E3})$$

where $\mathcal{H} = a'/a$ is the comoving Hubble parameter. The equation of motion [Eq. (E3)] is solved by separating h_{ij} into a vacuum mode $h_{ij}^{(0)}$, the solution of the homogeneous equation, and a sourced mode $h_{ij}^{(s)}$. The modes produced by the gauge quanta are statistically uncorrelated with those from the vacuum.

In the absence of a source, the power spectrum has the standard form

$$\mathcal{P}_h^{(0)} = \frac{2H^2}{\pi^2 M_{\text{pl}}^2}. \quad (\text{E4})$$

Since we are interested in superhorizon solutions for the sourced modes, we simply neglect the negative-helicity mode and the gradient term in the Fourier expansion of Eq. (E3). Then, the tensor mode is given by

$$h_+ \simeq \frac{-2S_{\text{eq}}}{M_{\text{pl}}^2 H^2} \mathcal{N}, \quad S_{\text{eq}} \simeq M_{\text{pl}}^2 H^2 \langle \mathcal{E}_i^2 \rangle_{\text{eq}}, \quad (\text{E5})$$

in which $\mathcal{N} \sim 60$ is the e -folding number of inflation and $\langle \mathcal{E}_i^2 \rangle_{\text{eq}}$ is defined in Eq. (3.33). Note that we work in the parameter space $1/2 < n < 2$ and have also neglected the contribution of magnetic fields due to the suppression factor ε^2 in Eq. (B19) in comparison to the electric part. Therefore, we find that

$$\mathcal{P}_h^{(s)} \simeq 4\mathcal{N}^2 \langle \mathcal{E}_i^2 \rangle_{\text{eq}}^2. \quad (\text{E6})$$

The two contributions add up in the power spectrum, yielding

$$\mathcal{P}_h = \mathcal{P}_h^{(0)} + \mathcal{P}_h^{(s)}. \quad (\text{E7})$$

Due to the production of the gauge quanta, the tensor-to-scalar ratio $r_t \equiv \mathcal{P}_h/\mathcal{P}_\zeta$ can be estimated as

$$r_t \simeq \frac{\mathcal{P}_h^{(0)}}{\mathcal{P}_\zeta} + \frac{4\mathcal{N}^2 \langle \mathcal{E}_i^2 \rangle_{\text{eq}}^2}{\mathcal{P}_\zeta}. \quad (\text{E8})$$

From CMB observations [67], the scalar power spectrum is given by $\mathcal{P}_\zeta \simeq 2.1 \times 10^{-9}$, while the constraint on the tensor-to-scalar ratio r_t is $r_t < 10^{-2}$. The above relation, along with Eq. (3.33) for $1/2 < n < 2$, besides the observational values for r_t and \mathcal{P}_ζ , leads to a relation for the Hubble parameter during inflation, which we denote by the dimensionless parameter h :

$$\frac{H}{M_{\text{pl}}} \equiv h(\xi, n, r_t). \quad (\text{E9})$$

For large enough ξ , we obtain $h \propto e^{-\pi\xi} (\mathcal{P}_\zeta r_t)^{1/4}$, which is consistent with Eq. (2.22). Having obtained the Hubble parameter during inflation, one can estimate the energy scale of inflation, defined as $\rho_{\text{inf}}^{1/4} \equiv (3M_{\text{pl}}^2 H^2)^{1/4}$. In Fig. 3, we have plotted the value of the inflationary energy scale as a function of ξ . We see that for $\xi > 4$, the energy scale of inflation decreases rapidly.

-
- [1] R. M. Kulsrud, R. Cen, J. P. Ostriker, and D. Ryu, *Astrophys. J.* **480**, 481 (1997).
- [2] S. Furlanetto and A. Loeb, *Astrophys. J.* **556**, 619 (2001).
- [3] I. B. Zeldovich, A. A. Ruzmaikin, and D. D. Sokolov, *flma* **3** (1983), <https://ui.adsabs.harvard.edu/abs/1983flma....3....Z/abstract>.
- [4] E. N. Parker, *Cosmical Magnetic Fields: Their Origin and Their Activity*, Oxford Classic Texts in the Physical Sciences (Oxford University Press, Oxford, United Kingdom, 2019).
- [5] M. Giovannini, *Classical Quant. Grav.* **35**, 084003 (2018).
- [6] K. Subramanian, *Rep. Prog. Phys.* **79**, 076901 (2016).
- [7] R. Durrer and A. Neronov, *Astron. Astrophys. Rev.* **21**, 62 (2013).
- [8] M. Giovannini, *Int. J. Mod. Phys. D* **13**, 391 (2004).
- [9] L. M. Widrow, *Rev. Mod. Phys.* **74**, 775 (2002).
- [10] T. Vachaspati, *Phys. Lett. B* **265**, 258 (1991).
- [11] M. Giovannini, *Classical Quant. Grav.* **13**, 135018 (2021).
- [12] M. Giovannini, *Eur. Phys. J. C* **81**, 81 (2021).
- [13] M. Giovannini, *Phys. Lett. B* **819**, 136444 (1991).
- [14] M. Giovannini, *Phys. Rev. D* **104**, 123509 (2021).
- [15] M. Giovannini, *J. Cosmol. Astropart. Phys.* **11** (2021) 058.
- [16] M. Giovannini, *J. Cosmol. Astropart. Phys.* **06** (2017) 017.
- [17] E. V. Gorbar, K. Schmitz, O. O. Sobol, and S. I. Vilchinskii, *Phys. Rev. D* **104**, 123504 (2021).
- [18] E. V. Gorbar, K. Schmitz, O. O. Sobol, and S. I. Vilchinskii, *arXiv:2111.04712*.
- [19] K.-W. Ng, S.-L. Cheng, and W. Lee, *Chin. J. Phys.* **53**, 110105 (2015).
- [20] K. Bamba, S. D. Odintsov, T. Paul, and D. Maity, *arXiv:2107.11524*.
- [21] D. Maity, S. Pal, and T. Paul, *J. Cosmol. Astropart. Phys.* **05** (2021) 045.
- [22] P. Vargas Moniz and J. Ward, *Class. Quant. Grav.* **27**, 235009 (2010).
- [23] M. S. Turner and L. M. Widrow, *Phys. Rev. D* **37**, 2743 (1988).
- [24] B. Ratra, *Astrophys. J.* **391**, L1 (1992).
- [25] D. Grasso and H. R. Rubinstein, *Phys. Rep.* **348**, 163 (2001).
- [26] T. Vachaspati, *Rep. Prog. Phys.* **84**, 074901 (2021).
- [27] R. Wiełebinski and R. Beck, *Cosmic Magnetic Fields* (Springer Science & Business Media, New York, 2005), Vol. 664.

- [28] A. Neronov and I. Vovk, *Science* **328**, 73 (2010).
- [29] K. Dolag, M. Kachelriess, S. Ostapchenko, and R. Tomas, *Astrophys. J.* **727**, L4 (2011).
- [30] W. Essey, S. Ando, and A. Kusenko, *Astropart. Phys.* **35**, 135 (2011).
- [31] A. M. Taylor, I. Vovk, and A. Neronov, *Astron. Astrophys.* **529**, A144 (2011).
- [32] C. Caprini and S. Gabici, *Phys. Rev. D* **91**, 123514 (2015).
- [33] L. Parker, *Phys. Rev. Lett.* **21**, 562 (1968).
- [34] B. Himmetoglu, C. R. Contaldi, and M. Peloso, *Phys. Rev. Lett.* **102**, 111301 (2009).
- [35] B. Himmetoglu, C. R. Contaldi, and M. Peloso, *Phys. Rev. D* **80**, 123530 (2009).
- [36] M. Gasperini, M. Giovannini, and G. Veneziano, *Phys. Rev. Lett.* **75**, 3796 (1995).
- [37] K. Bamba and J. Yokoyama, *Phys. Rev. D* **69**, 043507 (2004).
- [38] J. Martin and J. Yokoyama, *J. Cosmol. Astropart. Phys.* **01** (2008) 025.
- [39] V. Demozzi, V. Mukhanov, and H. Rubinstein, *J. Cosmol. Astropart. Phys.* **08** (2009) 025.
- [40] S. Kanno, J. Soda, and M.-a. Watanabe, *J. Cosmol. Astropart. Phys.* **12** (2009) 009.
- [41] R. Emami, H. Firouzjahi, and M. Movahed, *Phys. Rev. D* **81**, 083526 (2010).
- [42] T. Fujita and S. Mukohyama, *J. Cosmol. Astropart. Phys.* **10** (2012) 034.
- [43] M. Giovannini, *Phys. Rev. D* **87**, 083004 (2013).
- [44] T. Fujita and S. Yokoyama, *J. Cosmol. Astropart. Phys.* **09** (2013) 009.
- [45] R. J. Z. Ferreira, R. K. Jain, and M. S. Sloth, *J. Cosmol. Astropart. Phys.* **10** (2013) 004.
- [46] R. J. Z. Ferreira, R. K. Jain, and M. S. Sloth, *J. Cosmol. Astropart. Phys.* **06** (2014) 053.
- [47] T. Kobayashi, *J. Cosmol. Astropart. Phys.* **05** (2014) 040.
- [48] H. Bazrafshan Moghaddam, E. McDonough, R. Namba, and R. H. Brandenberger, *Classical Quant. Grav.* **35**, 105015 (2018).
- [49] O. O. Sobol, A. V. Lysenko, E. V. Gorbar, and S. I. Vilchinskii, *Phys. Rev. D* **102**, 123512 (2020).
- [50] N. Barnaby, R. Namba, and M. Peloso, *Phys. Rev. D* **85**, 123523 (2012).
- [51] R. Banerjee and K. Jedamzik, *Phys. Rev. D* **70**, 123003 (2004).
- [52] C. Caprini, M. C. Guzzetti, and L. Sorbo, *Classical Quant. Grav.* **35**, 124003 (2018).
- [53] C. Caprini and L. Sorbo, *J. Cosmol. Astropart. Phys.* **10** (2014) 056.
- [54] A. Talebian, A. Nassiri-Rad, and H. Firouzjahi, *Phys. Rev. D* **102**, 103508 (2020).
- [55] M.-a. Watanabe, S. Kanno, and J. Soda, *Phys. Rev. Lett.* **102**, 191302 (2009).
- [56] M.-a. Watanabe, S. Kanno, and J. Soda, *Prog. Theor. Phys.* **123**, 1041 (2010).
- [57] N. Bartolo, S. Matarrese, M. Peloso, and A. Ricciardone, *Phys. Rev. D* **87**, 023504 (2013).
- [58] R. Emami, H. Firouzjahi, S. M. Sadegh Movahed, and M. Zarei, *J. Cosmol. Astropart. Phys.* **02** (2011) 005.
- [59] R. Emami and H. Firouzjahi, *J. Cosmol. Astropart. Phys.* **10** (2013) 041.
- [60] R. Emami, H. Firouzjahi, and M. Zarei, *Phys. Rev. D* **90**, 023504 (2014).
- [61] R. Emami, Ph.D. thesis, Hong Kong University of Science and Technology, 2015.
- [62] A. A. Abolhasani, M. Akhshik, R. Emami, and H. Firouzjahi, *J. Cosmol. Astropart. Phys.* **03** (2016) 020.
- [63] T. Fujita and I. Obata, *J. Cosmol. Astropart. Phys.* **01** (2018) 049.
- [64] A. Talebian, A. Nassiri-Rad, and H. Firouzjahi, *Phys. Rev. D* **101**, 023524 (2020).
- [65] M. M. Anber and L. Sorbo, *J. Cosmol. Astropart. Phys.* **10** (2006) 018.
- [66] R. Durrer, L. Hollenstein, and R. K. Jain, *J. Cosmol. Astropart. Phys.* **03** (2011) 037.
- [67] Y. Akrami *et al.* (Planck Collaboration), [arXiv:1807.06211](https://arxiv.org/abs/1807.06211).
- [68] B. Salehian, M. A. Gorji, H. Firouzjahi, and S. Mukohyama, *Phys. Rev. D* **103**, 063526 (2021).
- [69] A. A. Starobinsky and J. Yokoyama, *Phys. Rev. D* **50**, 6357 (1994).
- [70] T. Fujita, M. Kawasaki, and Y. Tada, *J. Cosmol. Astropart. Phys.* **10** (2014) 030.
- [71] V. Vennin and A. A. Starobinsky, *Eur. Phys. J. C* **75**, 413 (2015).
- [72] M. Sasaki, Y. Nambu, and K.-I. Nakao, *Nucl. Phys.* **B308**, 868 (1988).
- [73] Y. Nambu and M. Sasaki, *Phys. Lett. B* **219**, 240 (1989).
- [74] K.-i. Nakao, Y. Nambu, and M. Sasaki, *Prog. Theor. Phys.* **80**, 1041 (1988).
- [75] L. Evans, An introduction to stochastic differential equations, *Miscellaneous Books* (American Mathematical Society, Providence, 2013).
- [76] P. P. Kronberg, *Rep. Prog. Phys.* **57**, 325 (1994).
- [77] G. B. Taylor and R. A. Perley, *Astrophys. J.* **416**, 554 (1993).
- [78] J. A. Eilek, [arXiv:astro-ph/9906485](https://arxiv.org/abs/astro-ph/9906485).
- [79] A.-C. Davis, M. Lilley, and O. Tornkvist, *Phys. Rev. D* **60**, 021301 (1999).
- [80] A. Brandenburg and K. Subramanian, *Phys. Rep.* **417**, 1 (2005).
- [81] P. P. Kronberg, M. L. Bernet, F. Miniati, S. J. Lilly, M. B. Short, and D. M. Higdon, *Astrophys. J.* **676**, 70 (2008).
- [82] M. L. Bernet, F. Miniati, S. J. Lilly, P. P. Kronberg, and M. Dessauges-Zavadsky, *Nature (London)* **454**, 302 (2008).
- [83] I. Vovk, A. M. Taylor, D. Semikoz, and A. Neronov, *Astrophys. J.* **747**, L14 (2012).
- [84] P. A. R. Ade *et al.* (Planck Collaboration), *Astron. Astrophys.* **594**, A19 (2016).
- [85] P. A. R. Ade *et al.* (POLARBEAR Collaboration), *Phys. Rev. D* **92**, 123509 (2015).
- [86] M. S. Pshirkov, P. G. Tinyakov, and F. R. Urban, *Phys. Rev. Lett.* **116**, 191302 (2016).
- [87] D. R. Sutton, C. Feng, and C. L. Reichardt, *Astrophys. J.* **846**, 164 (2017).
- [88] K. Jedamzik and A. Saveliev, *Phys. Rev. Lett.* **123**, 021301 (2019).
- [89] D. Paoletti, J. Chluba, F. Finelli, and J. A. Rubino-Martin, *Mon. Not. R. Astron. Soc.* **484**, 185 (2019).
- [90] J. D. Bray and A. M. M. Scaife, *Astrophys. J.* **861**, 3 (2018).

- [91] T. Fujita and R. Durrer, *J. Cosmol. Astropart. Phys.* **09** (2019) 008.
- [92] T. Fujita and S. Yokoyama, *J. Cosmol. Astropart. Phys.* **03** (2014) 013.
- [93] L. Campanelli, *Eur. Phys. J. C* **74**, 2690 (2014).
- [94] T. Kobayashi and M. S. Sloth, *Phys. Rev. D* **100**, 023524 (2019).
- [95] A. Kushwaha and S. Shankaranarayanan, *Phys. Rev. D* **102**, 103528 (2020).
- [96] A. Brandenburg, J. Schober, I. Rogachevskii, T. Kahniashvili, A. Boyarsky, J. Frohlich, O. Ruchayskiy, and N. Kleeorin, *Astrophys. J. Lett.* **845**, L21 (2017).
- [97] N. Barnaby, E. Pajer, and M. Peloso, *Phys. Rev. D* **85**, 023525 (2012).
- [98] N. Barnaby, R. Namba, and M. Peloso, *J. Cosmol. Astropart. Phys.* **04** (2011) 009.